Redox Biology 84 (2025) 103703

Contents lists available at ScienceDirect

Redox Biology

journal homepage: www.elsevier.com/locate/redox

Histone lactylation-induced premature senescence contributes to 1-nitropyrene-Induced chronic obstructive pulmonary disease

Rong-Rong Wang [a,b,1], Dan-Lei Chen [a,b,1], Meng Wei [c,1], Se-Ruo Li [a,b,1], Peng Zhou [a,b], Jing Sun [a,b], Qi-Yuan He [a,b], Jin Yang [a,b,**], Hui Zhao [a,b,d,***], Lin Fu [a,b,d,*]

[a] Department of Respiratory and Critical Care Medicine, The Second Affiliated Hospital of Anhui Medical University, Hefei, Anhui, 230601, China
[b] Institute of Respiratory Diseases, The Second Affiliated Hospital of Anhui Medical University, Hefei, Anhui, 230601, China
[c] Department of General Surgery, The First Affiliated Hospital of Anhui Medical University, Hefei, Anhui, 230022, China
[d] Center for Big Data and Population Health of IHM, The Second Affiliated Hospital of Anhui Medical University, Hefei, Anhui, 230601, China

ARTICLE INFO

Keywords:
1-Nitropyrene
COPD
Histone lactylation
P53
Cellular senescence

ABSTRACT

Our previous study revealed that mice exposed to 1-nitropyrene (1-NP) develop pulmonary fibrosis and senescent alveolar cells. However, the impacts of chronic 1-NP on chronic obstructive pulmonary disease (COPD) and the underlying mechanism are unclear. Our research suggested that chronic 1-NP evoked alveolar structure damage, inflammatory cell infiltration, and pulmonary function decline in mice. Moreover, 1-NP increased p53 and p21 expression, the number of β-galactosidase-positive cells, and cell cycle arrest in mouse lungs and MLE-12 cells. Moreover, 1-NP promoted glycolysis and upregulated lactic dehydrogenase A (LDHA) and lactate production in mouse lungs and MLE-12 cells. Elevated glycolysis provoked histone lactylation, but not histone acetylation in pulmonary epithelial cells. Mechanistically, histone H3 lysine 14 lactylation (H3K14la) was upregulated in pulmonary epithelial cells. *P53* knockdown mitigated 1-NP-induced cell cycle arrest and senescence in MLE-12 cells. CUT&Tag and ChIP-qPCR experiments confirmed that increased H3K14la directly upregulated *p53* transcription in pulmonary epithelial cells. As expected, *LDHA* knockdown alleviated 1-NP-triggered cell cycle arrest and senescence in MLE-12 cells. In addition, supplementation with oxamate, an inhibitor of LDH, attenuated 1-NP-incurred premature senescence and the COPD-like phenotype in mice. These data revealed for the first time that histone lactylation-induced the increase in p53 transcription contributes to pulmonary epithelial cell senescence during 1-NP-induced COPD progression. Our results provide a basis for repressing lactate production as a promising therapeutic strategy for COPD.

1. Introduction

1-Nitropyrene (1-NP) is a representative environmental pollutant belonging to the class of nitro polycyclic aromatic hydrocarbons (nitro-PAHs), primarily produced by the incomplete combustion of carbon-rich organic fuels, manufacturing, and mining [1,2]. 1-NP is also detected in rice grains, vegetables, river water, indoor kitchen air, dust, and the atmosphere [3-5]. 1-NP exposure occurs in the human body predominantly via the respiratory and digestive tracts, but dietary intake is one of the most frequent exposure routes [6-8]. Owing to its mutagenicity and carcinogenicity, 1-NP has been classified as a Group 2A carcinogen [9,10]. Previous studies have revealed that 1-NP exhibits reproductive and developmental toxicity and endocrine-disrupting activity [11-13]. Additionally, recent investigations have suggested that 1-NP exposure affects the respiratory system, evokes acute lung injury and pulmonary fibrosis, and increases the susceptibility to asthma in

* Corresponding author. Center for Big Data and Population Health of IHM, The Second Affiliated Hospital of Anhui Medical University, Hefei, Anhui, 230601, China.
** Corresponding author. Institute of Respiratory Diseases, The Second Affiliated Hospital of Anhui Medical University, Hefei, Anhui, 230601, China.
*** Corresponding author. Department of Respiratory and Critical Care Medicine, The Second Affiliated Hospital of Anhui Medical University, Hefei, Anhui, 230601, China.
E-mail addresses: yangqj1015@foxmail.com (J. Yang), zhaohuichenxi@126.com (H. Zhao), fulindev@126.com (L. Fu).
[1] The following authors contributed equally to this work.

https://doi.org/10.1016/j.redox.2025.103703
Received 27 March 2025; Received in revised form 17 May 2025; Accepted 26 May 2025
Available online 28 May 2025

adolescent offspring [14-16]. However, the influence of chronic 1-NP on chronic obstructive pulmonary disease (COPD) and the specific mechanism involved remain obscure.

COPD is typified by enduring respiratory difficulties and chronic inflammation which changes the structures of the lung parenchyma and peripheral airways and leads to significantly irreversible and progressive airflow limitation [17]. An epidemiological survey revealed that 544.9 million people experienced chronic respiratory diseases worldwide in 2017, and approximately half of the subjects progressed to COPD [18]. More recent research has shown that the total incidence of COPD is nearly one hundred million in Chinese adults [19]. Owing to the increasing aged population, COPD became the third most common cause of death globally and one of the main contributors to the disease burden [17,20]. To date, COPD is become a significant public health issue [21]. The traditional view has suggested that tobacco use is the main cause of COPD. However, an increasing number of environmental pollutants play important roles in COPD progression [22]. Although 1-NP exposure initiates a variety of respiratory diseases, reports on the link between 1-NP and COPD are scarce. Cellular senescence manifests as a prolonged cell cycle linked to alternations in cell morphology, secretory phenotype, telomere shortening, and epigenetics [23,24]. According to numerous research, cellular senescence can be divided into three categories: replicative senescence, premature senescence brought on by stress, and developmentally programmed cellular senescence [25,26]. Senescent cells secrete a plethora of factors, consisting of chemokines, cytokines, growth factors, and proteases, collectively called the senescence-associated secretory phenotype (SASP) [27]. The SASP mediates many pathophysiological effects, most of which are harmful to physical health [28]. Pulmonary epithelial cell senescence is involved in the initiation of COPD [29]. Our previous investigation has confirmed that 1-NP evokes alveolar cell senescence [30]. In addition, 1-NP exposure increases lactic dehydrogenase (LDH) levels in macrophages [31]. The most significant function of LDH is converting pyruvate to lactate and disrupting the cell redox balance [32]. Research has revealed that lactate binds to the lysine residues of histone and promotes histone lactylation. As a new epigenetic modification, histone lactylation increases gene transcription [33]. Moreover, histone lactylation regulates cellular senescence [34]. Overall, we hypothesize that 1-NP may induce COPD through histone lactylation-mediated pulmonary cell senescence.

Therefore, the intention of this finding was to assess the effects of chronic exposure to 1-NP on the premature senescence of pulmonary epithelial cells and COPD, as well as the underlying mechanisms involved. We assessed the impact of chronic 1-NP on cell cycle arrest and cellular senescence in both pulmonary epithelial cells and lung tissues. Additionally, the role of 1-NP treatment in regulating histone lactylation was examined in mouse lungs and pulmonary epithelial cells. Consequently, this study provides the first mechanistic explanation for chronic 1-NP-evoked COPD.

2. Materials and methods

2.1. Dose selection

A previous study has confirmed that the mice were exposed to 1-NP (5 μg) through intratracheal instillation for 29 times within four months, COPD-like phenotypes were observed in mice [35]. This meant that the chronic exposure of 145 μg 1-NP can evoke COPD model in mice within four months. However, the administration manner of intratracheal instillation is inconsistent with the exposure manner in the real world. Based on previous study from our research team, a non-invasive whole-body inhalation may be more suitable for the administration manner in the establishing process of COPD mouse model [36]. In the current research, the mice in the 1-NP group were exposed to 1-NP aerosol (200 mg/L) for 4 h per day, once every 2 days, for 16 weeks via a dynamic inhalation exposure chamber (DIEC). The total does of 1-NP deposition was calculated as following: 145 μg 1-NP = 24 mL/min $\times$ X μg/m^3 $\times$ 60 min $\times$ 4 h $\times$ 3 d $\times$ 16 w $\times$ 70 %== $24 \times 10^{-3} \times 10^{-3}$ m^3 /min $\times$ X μg/m^3 $\times$ 60 min $\times$ 4 h $\times$ 3 d $\times$ 16 w $\times$ 70 % [37]. According to the above data, the inhalation concentration of 1-NP is about 700 μg/m^3. Based on the parameters of the dynamic inhalation contamination device: Inlet airflow rate: 4.200 m^3/h; Drug concentration: 100 %; Drug density: 1040 mg/mL; Drug delivery rate: 0.404 mL/min; Total drug volume: 97.0 mL. Thus, the final concentration of 1-NP solution is about 200 mg/L in this study for animal experiments. Moreover, the previous studies have confirmed that cigarette smoke exposure induce a COPD model in mice for about four months [38,39]. After 16 weeks of exposure to 1-NP, pulmonary function was detected and the remaining mice were killed. The results indicated chronic exposure to 1-NP can incur a COPD-like phenotype in mice. According to the two reports from our team, we found that the concentration of 5 μM can incur cytotoxicity in pulmonary epithelial cells [16,30]. Therefore, the concentration of 5 μM was selected for cellular experiment.

2.2. Animal models and treatments

Beijing Vital River provided the male C57BL/6 mice, which were six weeks old. Every mouse was raised in a specific pathogen-free (SPF) animal facility with controlled temperature and light, and had free access to food and water. Two independent animal experiments were involved in this study:

In Experiment 1, we assessed the impacts of chronic 1-NP treatment on COPD in mice. Mice were randomly assigned to either the 1-NP or control (Ctrl) group. Mice in the 1-NP group were exposed to 1-NP aerosol (700 μg/m^3) for 4 h per day, three days a week, via a dynamic inhalation exposure chamber (DIEC). Control mice were subjected to the same conditions but received DMSO exposure under standard housing conditions.

In Experiment 2, we aimed to investigate the impact of lactylation on cellular senescence and COPD. Mice were assigned to different groups: Ctrl, oxamate (OXA), 1-NP, and OXA+1-NP. Mice in the OXA and OXA+1-NP groups received an intraperitoneal injection of OXA (100 mg/kg) before 1-NP exposure. Mice were exposed to 1-NP aerosol (700 μg/m^3) in the 1-NP and OXA+1-NP groups for 4 h per day, five days a week.

After 16 weeks of exposure to 1-NP, pulmonary function was assessed. The animals were then euthanized, and blood and lung tissues were harvested. For histological analysis, the left lung was preserved in 4 % paraformaldehyde solution, and the right lung was stored in liquid nitrogen for subsequent experiments.

2.3. Examination of pulmonary function

Pulmonary function was assessed via the AniRes 2005 lung function system (Beijing, China). Following anesthesia, the trachea of each mouse was carefully exposed, and a catheter was securely inserted into the trachea, connecting it to the pulmonary function analyzer. Measurements were performed under either pressure control or volume control modes. Key parameters, including forced vital capacity (FVC), forced expiratory volume in 1 s (FEV1), and the FEV1/FVC ratio, were recorded.

2.4. Treatments and cell cultures

The American Type Culture Collection (USA) provided the mouse lung epithelial (MLE)-12 cells, which were cultivated in DMEM with 10 % FBS. The cells were maintained in a temperature-controlled incubator at 37 °C with 5 % CO_2. This investigation involved two separate cellular experiments.

(1) To observe the influence of acute 1-NP on cellular senescence and lactylation, MLE-12 cells were cocultured with 1-NP (5 μM). MLE-

12 cells were gathered at diverse times after 1-NP coculture, and markers of cellular senescence and lactylation were detected.

(2) To evaluate the role of lactylation on cellular senescence, LDHA siRNA (siLDHA) was used to repress the expression of LDHA in MLE-12 cells. siLDHA plasmids were transfected into MLE-12 cells before 1-NP. Twenty-four hours after siLDHA transfection, the cells were cocultured with 1-NP (5 μM) for varying durations. The siRNA sequences were shown in Supplemental Table 1.

2.5. Extraction of protein and western blotting

Lung tissues or MLE-12 cells were lysed with RIPA buffer supplemented with protease and phosphatase inhibitors. The lysates were centrifuged and then the supernatants were obtained. The protein concentrations were ascertained via a BCA protein assay kit. Proteins in equal quantities were subsequently isolated via SDS-PAGE and transferred to a PVDF membrane. After blocking the membrane with nonfat milk, primary antibodies were incubated at 4 °C for one night. After being washed, the membrane was subsequently incubated with secondary antibodies conjugated to horseradish peroxidase. Protein bands were then visualized using an enhanced chemiluminescence detection system. The primary antibodies used were shown in Supplemental Table 2.

2.6. Reverse transcription (RT)-qPCR

TRIzol reagent was used to extract total RNA from mouse lungs or MLE-12 cells. The extraction process involved chloroform separation, followed by isopropanol precipitation and purification with 75 % ethanol. cDNA synthesis was performed using a commercial reverse transcription kit (Takara, Cat# RR036A). Primers specific to this study were designed with the NCBI Primer Design Tool (Supplemental Table 3). The cDNA, TB Green Master Mix (Takara, Cat# RR820A), and primers were combined and subjected to quantitative PCR analysis. Gene expression levels were determined by calculating the threshold cycle (CT) values.

2.7. Senescence-associated beta-galactosidase (SA-β-gal) staining

In brief, MLE-12 cells or frozen sections of mouse lungs were washed in PBS and subsequently fixed in β-galactosidase staining solution for 15 min at room temperature. After that, the cells or sections were cleaned with PBS, stained using a Beyotime C0602 kits, and sealed with sealing film. The positive cells were visible under a microscope during an overnight incubation at 37 °C until the color was changed to blue.

2.8. Flow cytometry

A Cell Cycle and Apoptosis Analysis Kit (Beyotime, Cat# C1052) was used. First, MLE-12 cells were collected and dissociated via trypsin. Following a 70 % ethanol fixation, the cells were cleaned and resuspended in PBS. Subsequently, the cells were subjected to propidium iodide staining solution for the detection of the DNA content. The cells were incubated for 30 min at 37 °C in the dark and then stored at 4 °C. Finally, flow cytometry was used to analyze the red fluorescence and light scattering of the cells at an excitation wavelength of 488 nm to assess the DNA content and cellular senescence.

2.9. Lactate level detection

Lung tissues, serum samples, or MLE-12 cells were ultrasonically sonicated on ice for 5 min, followed by 10 min of centrifugation at 4 °C and 12000 rpm. The supernatant was collected, and the concentration of lactate was determined via a Lactate Assay Kit (Solarbio, BC2230) following the guidelines provided by the manufacturer.

2.10. Histone protein extraction

Histone protein was extracted from MLE-12 cells or lung tissues via the EpiQuik Total Histone Extraction Kit (Epigentek Group, Inc., Catalog# OP-0006). To extract histones from MLE-12 cells or lung tissues, prelysis buffer was added to lyse the samples at 0∼4 °C. After centrifuging the homogenized materials for 5 min at 3000 rpm, the supernatants were gathered. The cell or tissue supernatants were resuspended in 3 vol of lysis buffer and dissociated. After centrifugation, the supernatant was obtained for subsequent western blotting.

2.11. Histological analysis, immunohistochemistry (IHC), and immunofluorescence (IF)

7. In short, fresh lung tissues were embedded in paraffin, fixed with 4 % paraformaldehyde for a whole night, and then sliced into 5-μm-thick sections. For histopathological evaluation, these sections were stained with hematoxylin-eosin (H&E). The degree of pulmonary injury was estimated by the pathological score. According to the criteria of the American Thoracic Society, neutrophil infiltration, thickness of alveolar and alveolar congestion are used to evaluate the severity of pulmonary injury [40]. For IHC, the sections were incubated with primary and secondary antibodies at 4 °C. The color reaction was determined via the use of an HRP-linked polymer. For IF, MLE-12 cells or frozen sections of lung tissues were fixed for 20 min with 4 % paraformaldehyde, permeabilized for 30 min at room temperature with 3 % Triton X-100, then blocked for 30 min at room temperature with 10 % goat blocking serum. The cells or lung sections were subsequently incubated with primary and fluorescent secondary antibodies overnight. DAPI staining was used for nuclear visualization. Finally, the positive cells or nuclei were counted via a Zeiss microscope.

2.12. CUT&Tag

The cells were collected and counted at room temperature using a Countstar Rigel S2 (Shanghai Ruiyu, FL20447, CHINA). The cells were lysed for 5 min, after which the cellular nuclei were extracted. The cellular nuclei were used to bind to the ConA beads. Then, the primary and secondary antibodies were treated with the attached cellular nuclei. Then, the bound nuclei were cultivated with the pA/G-transposome adapter complex, and the transposase was activated. The genomic DNA was liberated by proteinase K digestion and retrieved. Next, the genomic DNA was exposed to PCR amplification and purification. Library fragments of approximate 200-700 bp were obtained through bead selection. The concentration of the library fragments was measured via a Qubit instrument (Thermo, Qubit 3.0, USA), and the integrity of the fragments was assessed via a Bioanalyzer 2100 instrument (Agilent, CA, USA). PE150 sequencing was performed via the Illumina NovaSeqXP according to standard protocols.

2.13. Chip-qPCR

After the treatment of MLE-12 cells, the samples were treated with 125 mM glycine for 5 min at room temperature after being cross-linked for for 10 min with 1 % formaldehyde. After three rounds of cold PBS washing, the cells were scraped and centrifuged at 4 °C to remove the supernatants. The chromatin DNA was then sheared by sonicating the nuclei after they had been treated with nuclear lysis buffer. We designated 10 % of the sonicated chromatin as the "input" sample. The remaining 80 % underwent immunoprecipitation using an anti-H3K14la antibody (PTM-1414RM, PTM BIO, China) and was named as "IP". As a negative control, 10 % was treated with rabbit IgG (Cell Signaling Technology), which was referred to as "IgG". The phenol-chloroform extraction procedure was used to extract DNA from the input and IP samples respectively. Using the VAHTS Universal DNA Library Prep Kit for Illumina V3 (Catalog No. ND607, Vazyme), the DNA sequencing

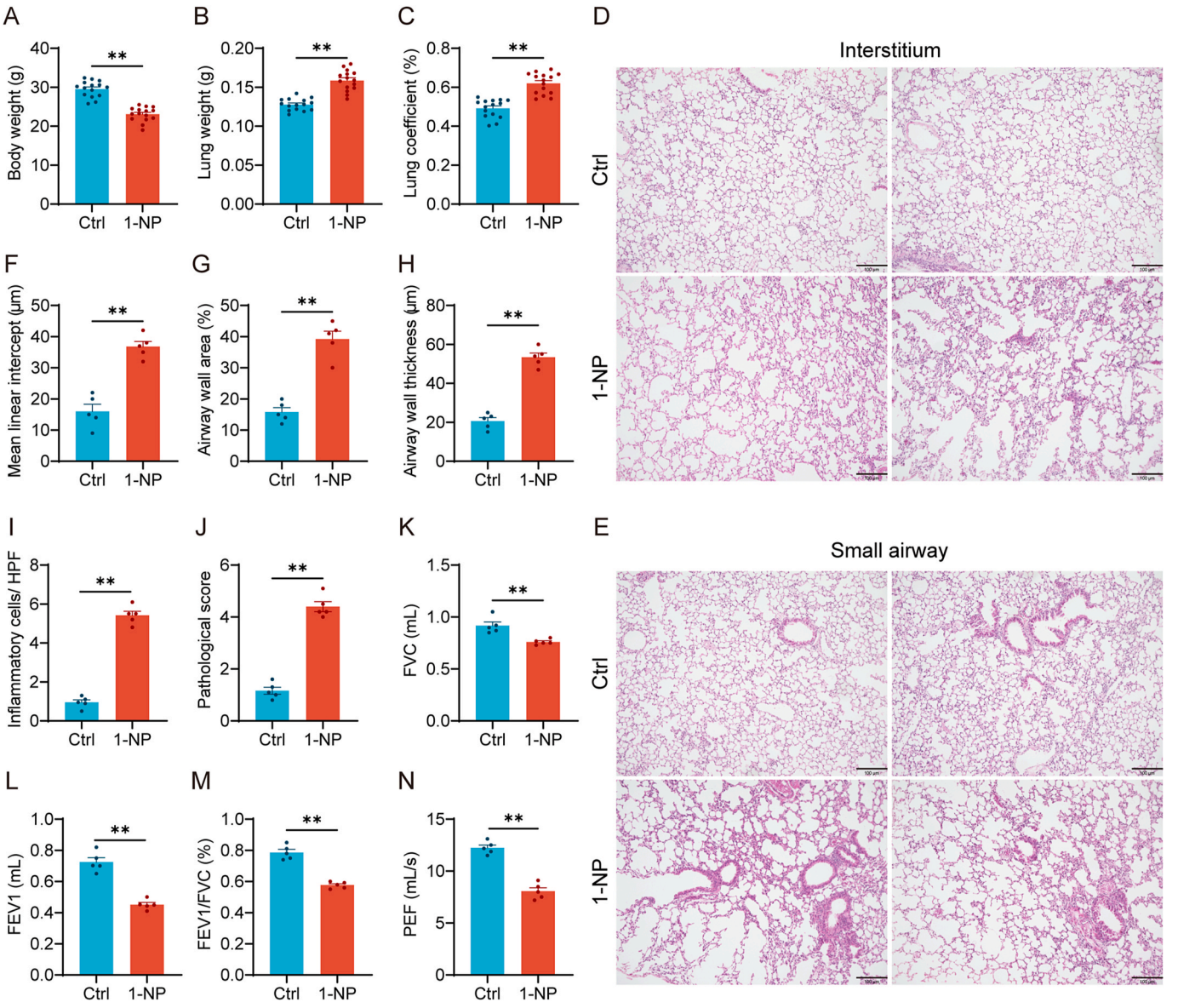

Fig. 1. 1-NP exposure caused a COPD-like phenotype in mice. (A-N) All the mice were exposed to 1-NP aerosol (200 mg/L, 4 h/day, once every 2 days) or DMSO through the respiratory tract for 4 months. All the mice were harvested, and pulmonary function was detected. (A) Body weight. (B) Lung weight. (C) Lung coefficient. (D, E) Lung sections were stained with hematoxylin and eosin. Original magnification: 100 × . (D) Pulmonary interstitium. (E) Pulmonary small airway. (F) Mean linear intercept. (G) Airway wall area. (H) Airway wall thickness. (I) Inflammatory cells. (J) Pathological scores. (K-N) Pulmonary function was measured. (K) FVC. (L) FEV1. (M) FEV1/FVC. (N) PEF. All the data were expressed as the means ± S.E.M. (N=5). *$P < 0.05$, **$P < 0.01$.

libraries were created. The DNBSEQ-T7 sequencer (MGI Tech Co., Ltd., China) was used to enrich, quantify and sequence the libraries with 200-500 bp fragments in PE150 mode. The primer sequence for ChIP-qPCR was as follows: *p53*, *5'-ACTGTGTGTGATGAGTGACG-3' 3'- AAGATAACCAGAGGCACTTCC-5'*.

2.14. Case-control study

In order to compare the proteins expressions of H3K14la and p53 in lung tissues of COPD patients and control subjects, a case-control was designed and executed. COPD patients were diagnosed on the basis of the diagnostic criteria and lung tissues were collected [41]. According to the previous studies, control subjects were selected from paracancerous tissues in lung cancer patients without other pulmonary diseases, and matched by gender and age with COPD cases [42,43]. All volunteers were selected in the Second Affiliated Hospital of Anhui Medical University. The clinical characteristics and demographic information were compared and represented in Supplemental Table 4. The expressions of H3K14la and p53 were detected in lung tissues and the relationship was evaluated.

2.15. Statistical analysis

Data analysis was executed by GraphPad Prism software (version 9.5.0; GraphPad Inc., located in San Diego, California, USA). Results were displayed in the form of mean ± standard error of the mean (SEM). When assessing data between two groups, the student t-test was adopted. For comparing data among multiple groups, one-way ANOVA was applied, followed by Tukey's post-hoc test. Moreover, the associations between p53 and H3K14la were estimated in COPD patients and control subjects via Pearson correlative analysis. Statistical significance was determined as a P value < 0.05. All experiments were conducted biologically for at least three times.

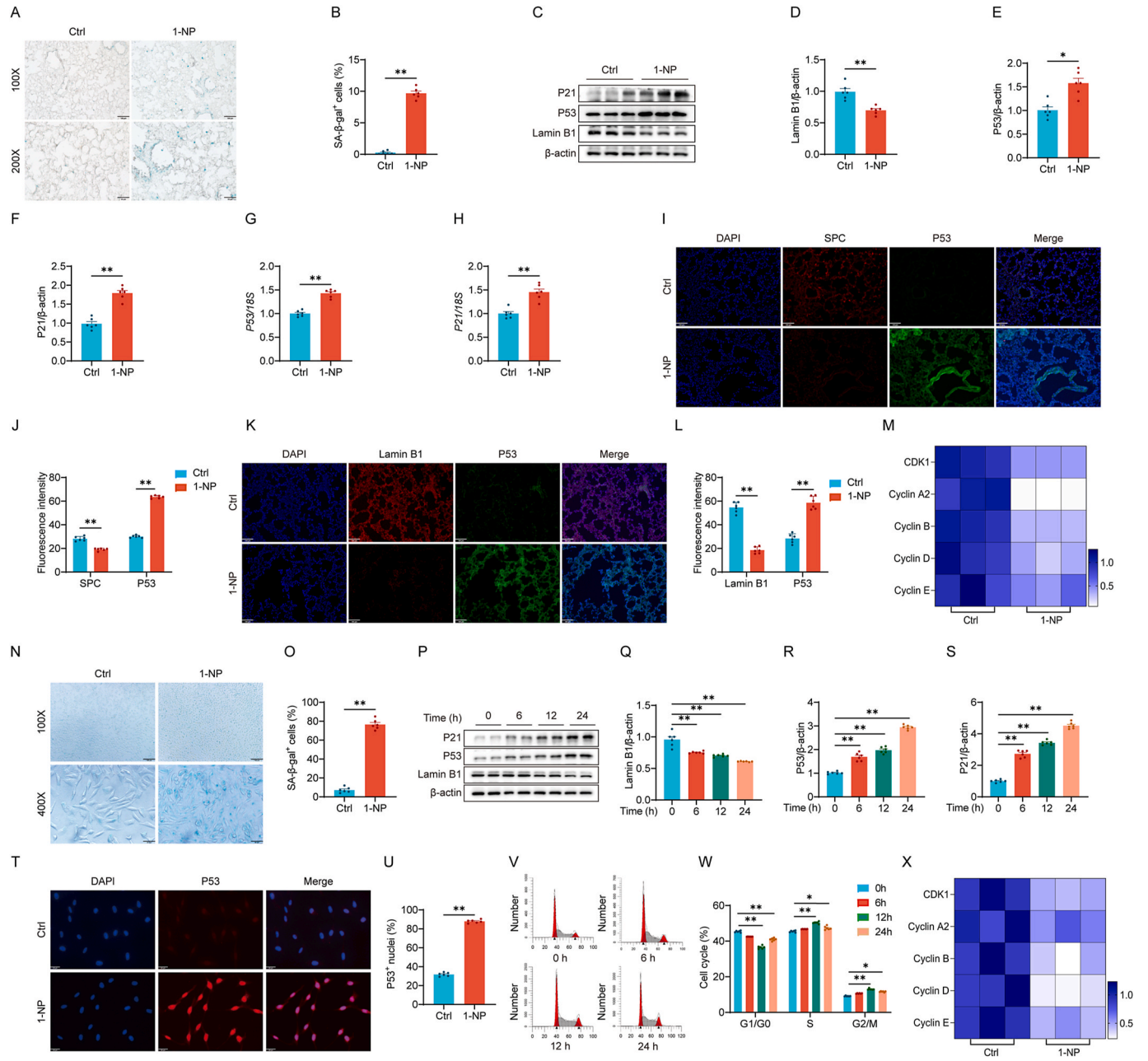

Fig. 2. 1-NP exposure induced cell cycle arrest and premature senescence in mouse lungs and MLE-12 cells. (A-K) All the mice were exposed to 1-NP aerosol (200 mg/L, 4 h/day, once every 2 days) or DMSO through the respiratory tract for 4 months. All the mice were harvested, and cell cycle arrest and cellular senescence were evaluated. (A) Lung sections were stained with SA-β-gal. Original magnification: 100 × and 200 × . (B) The number of SA-β-gal-positive cells was calculated. (C) The protein expression of cellular senescence markers was assessed via western blotting. (D-F) Quantitative analyses were conducted. (D) Lamin B1. (E) P53. (F) P21. (G-H) The mRNA levels of senescence markers were detected via RT-qPCR. (G) *P53*. (H) *P21*. (I, J) The colocalization of SPC with p53 was evaluated by IF. (I) Representative images were shown. Original magnification: 100 ×. (J) The number of colocalized cells was evaluated. (K, L) The colocalization of Lamin B1 with p53 was evaluated by IF. (K) Representative images were shown. Original magnification: 100 ×. (L) The number of colocalized cells was evaluated. (M) The mRNA levels of cyclins and cyclin-dependent kinases were detected via RT-qPCR. (N-X) MLE-12 cells were treated with 1-NP (5 μm) for different durations. Then, cell cycle arrest and senescence were evaluated. (N) SA-β-gal staining was performed in MLE-12 cells. Original magnification: 100 × and 400 × . (O) The number of SA-β-gal-positive cells was calculated. (P) The protein expression of cellular senescence markers was assessed with western blotting. (Q-S) Quantitative analyses were conducted. (Q) Lamin B1. (R) P53. (S) P21. (T) p53-positive nuclei were detected via IF. Original magnification: 630 × . (U) The number of p53-positive nuclei was assessed. (V) Cell cycle distribution was measured via flow cytometry. (W) Cell cycle distribution was analyzed. (X) Cyclin and cyclin-dependent kinases mRNA levels were detected via RT-qPCR. All the data were expressed as the means ± S.E.M. (N=6). $^{*}P < 0.05$, $^{**}P < 0.01$.

3. Results

3.1. Chronic 1-NP exposure caused a COPD-like phenotype in mice

Chronic 1-NP treatment prominently decreased body weight and increased the lung weight and lung coefficient in mice (Fig. 1A-C). In addition, chronic 1-NP evoked sensible lung injury, structural changes in the interstitium and small airway, and inflammatory cell infiltration (Fig. 1D, E). Quantitative analysis revealed that the lung tissues of mice had a higher mean linear intercept after 1-NP (Fig. 1F). In addition, chronic 1-NP exposure increased the airway wall area and airway wall thickness in the lungs of the mice (Fig. 1G, H). Moreover, the number of

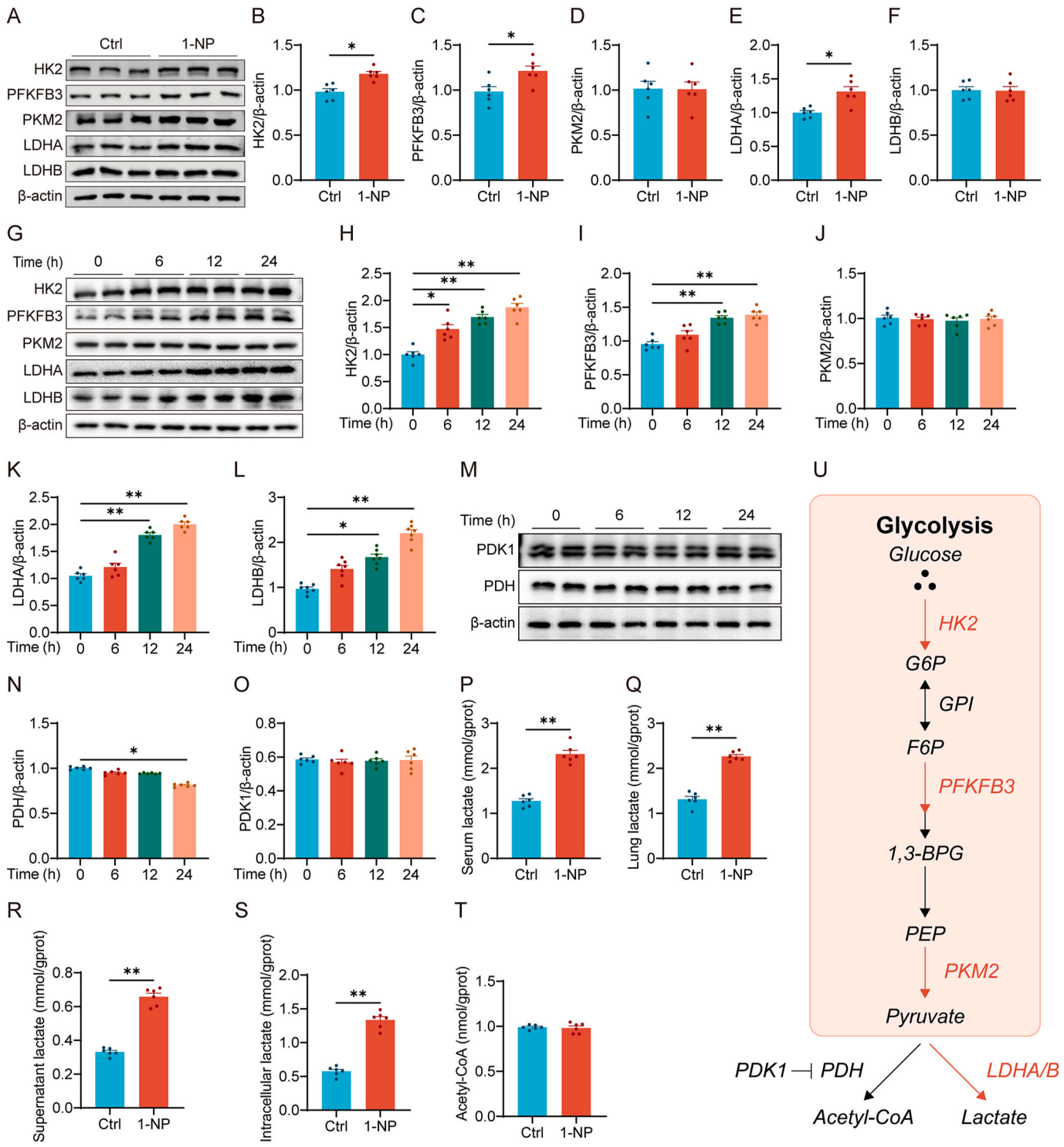

Fig. 3. 1-NP exposure incurred glycolysis and lactate production in mouse lungs and MLE-12 cells. (A-F) All the mice were exposed to 1-NP aerosol (200 mg/L, 4 h/day, once every 2 days) or DMSO through the respiratory tract for 4 months. All the mice were harvested, and the protein expression of glycolysis-related genes in mouse lungs was assessed via western blotting. (A) Representative bands were shown. (B-F) Quantitative analyses were conducted. (B) HK2. (C) PFKFB3. (D) PKM2. (E) LDHA. (F) LDHB. (G-L) MLE-12 cells were treated with 1-NP (5 μm) for different durations. The expression levels of glycolytic enzymes were subsequently measured. (G) Representative bands were shown. (H-L) Quantitative analyses were conducted. (H) HK2. (I) PFKFB3. (J) PKM2. (K) LDHA. (L) LDHB. (M – O) The key enzyme involved in the conversion of pyruvate to acetyl-CoA and its inhibitor were assessed via western blotting. (M) Representative bands were shown. (N, O) Quantitative analyses were conducted. (N) PDH. (O) PDK1. (P-S) Lactate levels were detected. (P) Serum lactate. (Q) Pulmonary lactate. (R) Supernatant lactate. (S) Intracellular lactate. (T) The content of intracellular acetyl-CoA was measured in MLE-12 cells. (U) Schematic of glycolysis. All the data were expressed as the means ± S.E.M. (N=6). $^{*}P < 0.05$, $^{**}P < 0.01$.

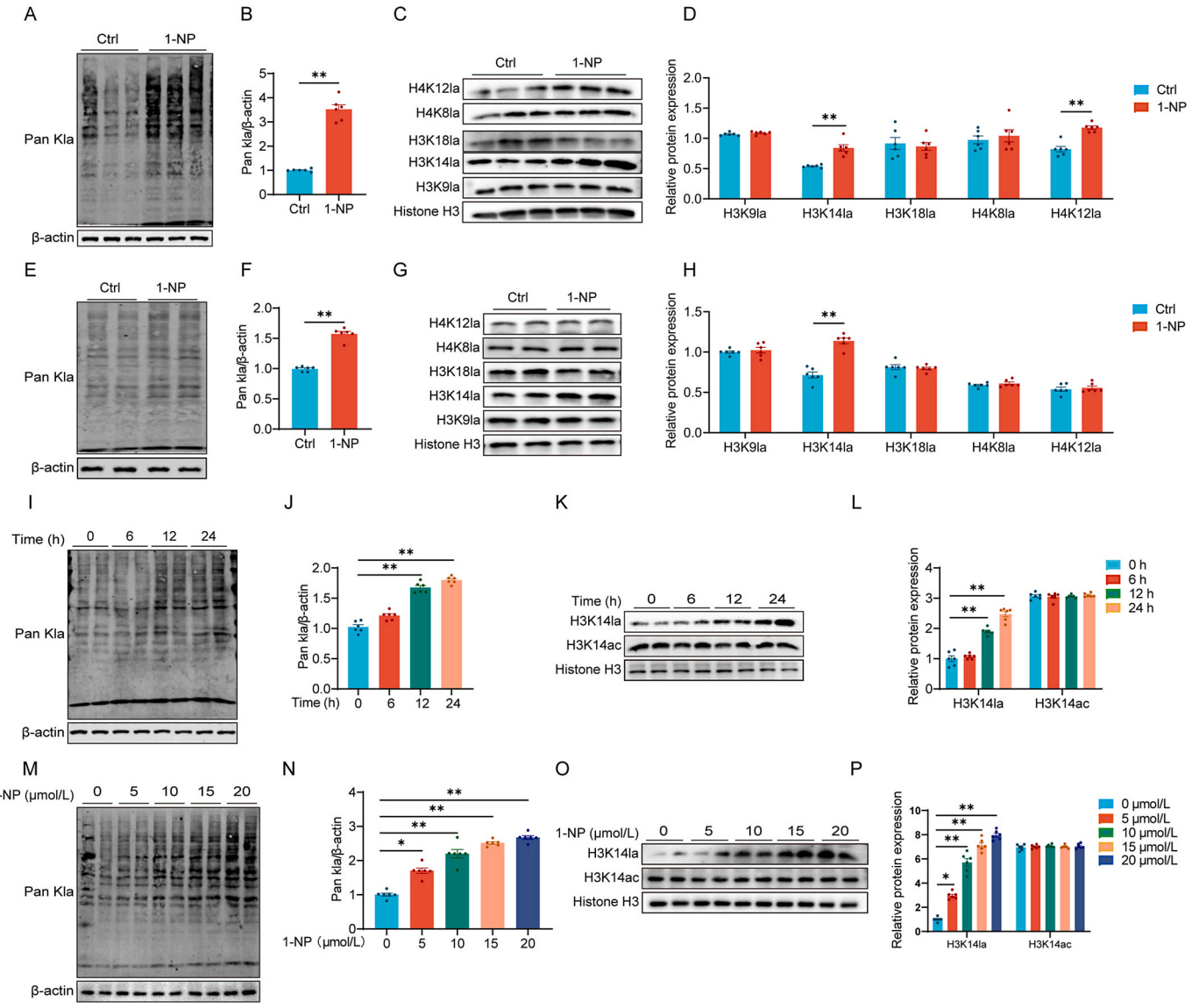

Fig. 4. 1-NP exposure promoted histone lactylation in mouse lungs and MLE-12 cells. (A-D) All the mice were exposed to 1-NP aerosol (200 mg/L, 4 h/day, once every 2 days) or DMSO through the respiratory tract for 4 months. All the mice were harvested and histone lactylation in mouse lungs was evaluated. (A) Pan Kla levels were measured via western blotting. (B) Quantitative analysis was conducted. (C) Different histone lactylation levels were determined by western blotting. (D) Quantitative analyses were performed. (E-H) MLE-12 cells were treated with 1-NP (5 μm) for 24 h. (E) Pan Kla was detected via western blotting. (F) Quantitative analysis was performed. (G) The levels of different types of histones lactylation were evaluated via western blotting. (H) Quantitative analyses were performed. (I-L) The effects of 1-NP exposure (5 μm) on histone lactylation and acetylation were explored in MLE-12 cells at 0 h, 6 h, 12 h, and 24 h. (I) Pan Kla was detected via western blotting. (J) Quantitative analysis was performed. (K) H3K14la and H3K14ac expression was determined via western blotting. (L) Quantitative analyses were performed. (M − P) Effects of 1-NP exposure at different concentrations (0 μmol/L, 5 μmol/L, 10 μmol/L, 15 μmol/L, and 20 μmol/L) on histone lactylation and acetylation were analyzed in MLE-12 cells after 24 h. (M) Pan Kla expression was determined via western blotting. (N) Quantitative analysis was performed. (O) H3K14la and H3K14ac protein expressions levels were evaluated via western blotting. (P) Quantitative analyses were performed. All the data were expressed as the means ± S.E.M. (N=6). $^{*}P < 0.05$, $^{**}P < 0.01$.

inflammatory cells per high-power field (HPF) and pathological scores in mouse lungs were significantly elevated following 1-NP exposure (Fig. 1I, J). Finally, the influence of long-term exposure to 1-NP on pulmonary function was evaluated. As shown in Fig. 1K-N, FEV1, FVC, FEV1/FVC, and peak expiratory flow (PEF) noticeably decreased in the 1-NP-exposed mice. Moreover, the types of infiltrated inflammatory cells were evaluated. The results suggested that chronic 1-NP exposure elevated the numbers of neutrophils and macrophages in mouse lungs (Supplemental Fig. 1A–D). Additionally, extracellular matrix (ECM) collagen was obviously deposited around the small airways in mouse lungs (Supplemental Fig. 1E and F). Besides, 1-NP increased collagen deposition in mouse lungs (Supplemental Fig. 1G and H). In addition, chronic 1-NP exposure inhibited the expression of E-cadherin, an epithelial marker, and promoted the expression of N-cadherin and vimentin, two mesenchymal indices, in lung tissues (Supplemental Fig. 1I–L).

3.2. *Chronic 1-NP exposure induced cell cycle arrest and senescence in pulmonary epithelial cells*

The effect of chronic 1-NP exposure on cellular senescence was estimated in mouse lungs. As shown in Fig. 2A and B, a greater number of SA-β-gal-positive cells in the lungs of the mice was caused by long-term exposure to 1-NP. In addition, the expression of Lamin B1, an intracellular marker of cellular senescence, was reduced in mouse lungs in the 1-NP group (Fig. 2C, D). P53 is a tumor suppressor that regulates

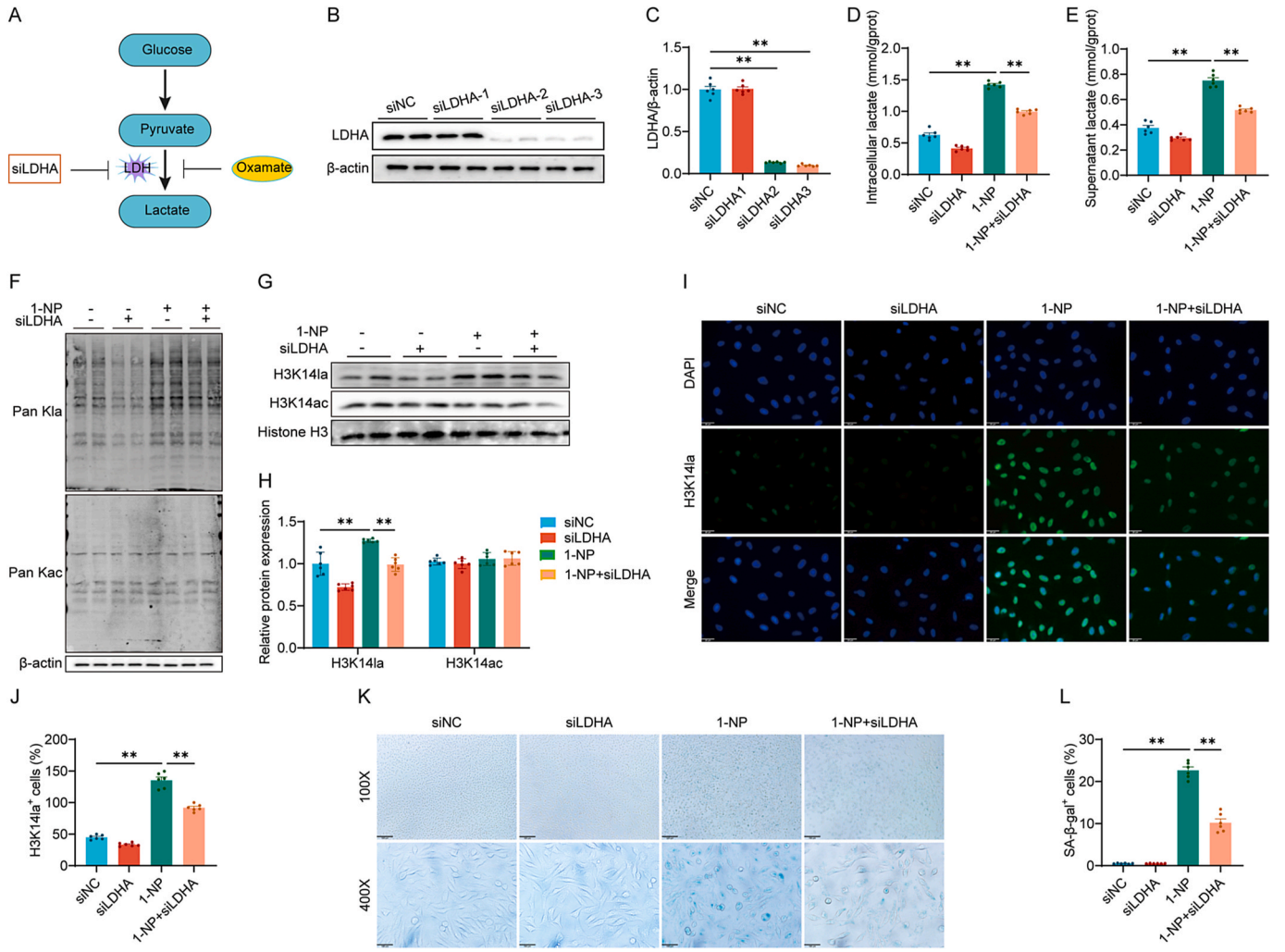

Fig. 5. *LDHA* knockdown alleviated histone lactylation, cell cycle arrest, and premature senescence in MLE-12 cells. (A) Diagrammatic sketch of lactate production. (B-J) The impact of *LDHA* knockdown on 1-NP-mediated histone lactylation was analyzed in MLE-12 cells. *LDHA* siRNAs were transfected, and then, MLE-12 cells were cocultured with 1-NP (5 μM). (B, C) LDHA protein expression was measured via western blotting. (D) The content of intracellular lactate was measured. (E) Lactate levels in the supernatant were determined. (F) Pan Kla and Pan Kac proteins expression was measured via western blotting. (G) H3K14la and H3K14ac proteins expression was measured via western blotting. (H) Quantitative analyses were performed. (I, J) H3K14la-positive nuclei were identified via IF and analyzed. Original magnification: 400 ×. (K-W) The influences of *LDHA* knockdown on 1-NP-evoked cell cycle arrest and premature senescence were explored in MLE-12 cells. (K) Senescent cells were evaluated by SA-β-gal staining. Original magnifications: 100 × and 400 × . (L) The number of SA-β-gal-positive cells was calculated. (M) The protein expression of cell cycle markers was detected via western blotting. (N-P) Quantitative analyses were performed. (N) Lamin B1. (O) P53. (P) P21. (Q, R) *p53* and *p21* mRNA levels were detected via RT-qPCR. (Q) *P53*. (R) *P21*. (S) P53-positive nuclei were tested by IF. Original magnification: 400 ×. (T) The number of p53-positive nuclei was calculated. (U) The cell cycle distribution was determined by flow cytometry. (V) Cell cycle distribution was analyzed. (W) The mRNA levels of SASP genes were detected by RT-qPCR. All the data were expressed as means ± S.E.M. (N=6). $^{*}P < 0.05$, $^{**}P < 0.01$.

the cell cycle, and p21 is a cyclin-dependent kinase inhibitor that is activated by p53 to halt the cell cycle. As expected, the protein and mRNA levels of p21 and p53 were elevated in the lungs of 1-NP-treated mice (Fig. 2C, 2E-H). Besides, 1-NP treatment substantially promoted the colocalization of surfactant protein C (SP-C), the marker of alveolar type II cells, with p53 in mouse lungs (Fig. 2I, J). Not only that, 1-NP exposure promoted the colocalization between Lamin B1 and p53 in mouse lungs (Fig. 2K, L). Moreover, the mRNA levels of cyclins and cyclin-dependent kinases were decreased in mice after chronic 1-NP (Fig. 2M). Additionally, 1-NP treatment markedly increased the mRNA expression levels of SASP genes in the lungs, including chemokines (*Cxcl1*, *Ccl2*, *Cxcl9*), metalloproteinases (*Mmp2*, *Mmp7*, *Mmp13*), and cytokines (*Il-1β*, *Il-6*, *Tnf-α*) (Supplemental Fig. 2A). These results revealed that chronic 1-NP induced cell cycle arrest and senescence in the alveolar type II cells of the mice. The effect of 1-NP treatment on cellular senescence was then examined in MLE-12 cells. The results indicated that chronic 1-NP cultivation increased the number of SA-β-gal-positive MLE-12 cells (Fig. 2N, O). Additionally, 1-NP exposure reduced Lamin B1 expression and upregulated p53 and p21 expressions in MLE-12 cells (Fig. 2P-S). IF also confirmed that the number of p53-positive nuclei was increased after 1-NP (Fig. 2T, U). Flow cytometry revealed that 1-NP led to a decrease in the proportion of MLE-12 cells in the G0/G1 phase, whereas the proportions of those in the S and G2/M phases increased, indicating that cell cycle arrest occurred in the S and G2/M phases (Fig. 2V, M). Not only that, the mRNA levels of cyclins and cyclin-dependent kinases in MLE-12 cells were decreased after 1-NP (Fig. 2X), whereas the expression of SASP mRNAs were increased (Supplemental Fig. 2B).

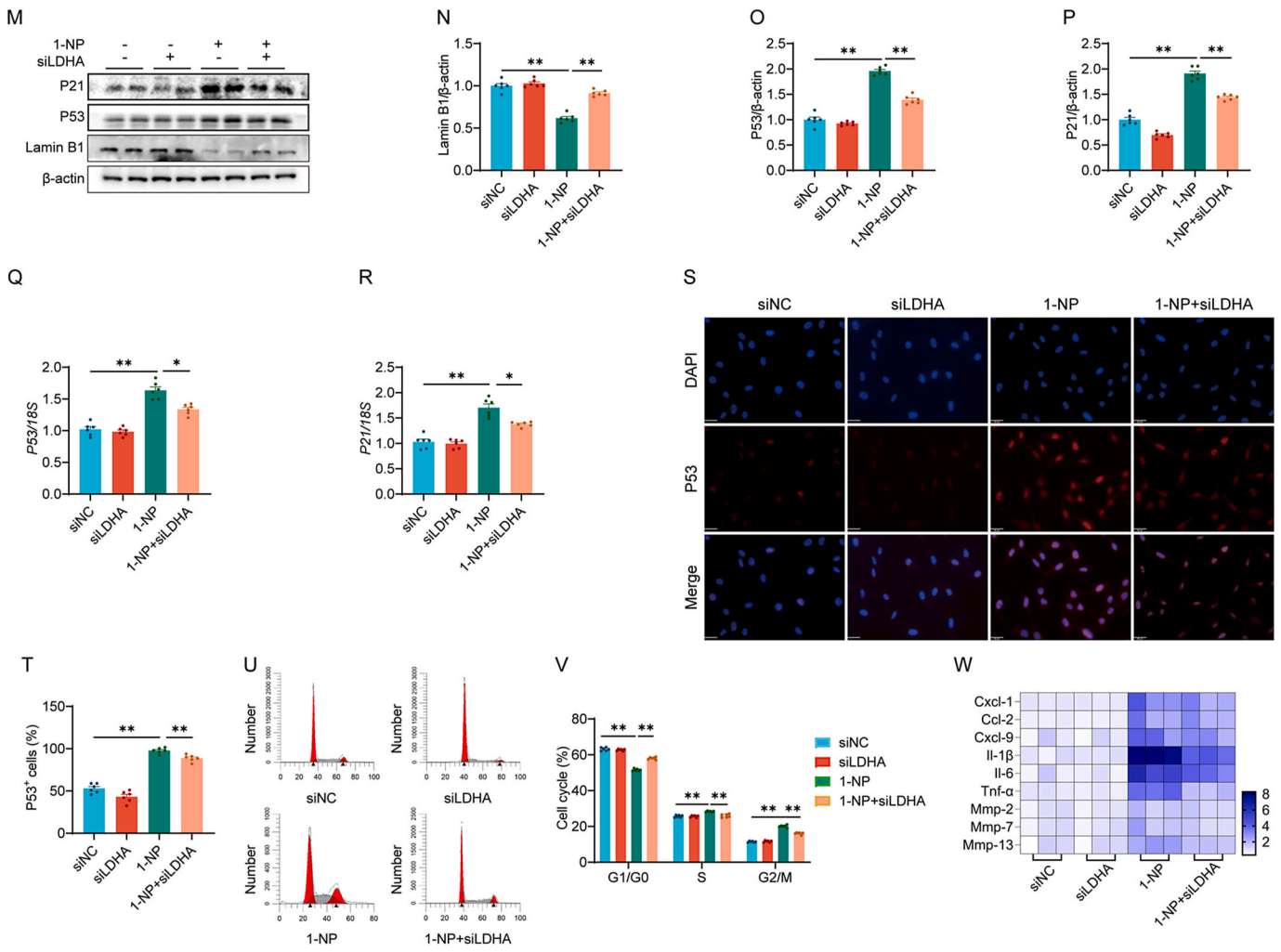

Fig. 5. (*continued*).

3.3. 1-NP exposure promoted glycolysis and lactate production in pulmonary epithelial cells

The impacts of chronic 1-NP exposure on glycolysis and lactate production were evaluated in mouse lungs. As shown in Fig. 3A-D, three key glycolytic enzymes, hexokinase 2 (HK2) and phosphofructokinase 2 (PFKFB3) were significantly elevated in mouse lungs following 1-NP exposure. Surprisingly, 1-NP exposure didn't affect the pyruvate kinase M2 (PKM2) expression in mouse lungs. Chronic 1-NP increased the expression of lactate dehydrogenase A (LDHA), which is a crucial enzyme for lactate production (Fig. 3A, E). However, chronic 1-NP did not influence LDHB expression (Fig. 3A, F). Additionally, acute 1-NP treatment upregulated HK2, PFKFB3, LDHA, and LDHB expressions in MLE-12 cells (Fig. 3G-L). Pyruvate dehydrogenase (PDH), which converts pyruvate to acetyl-CoA, was reduced in MLE-12 cells treated with 1-NP (Fig. 3M, N), whereas its inhibitor, pyruvate dehydrogenase kinase 1 (PDK1), remained unchanged after 1-NP (Fig. 3M, O). Additionally, chronic 1-NP promoted lactate production in serum and lung tissues of mouse (Fig. 3P, Q). As expected, lactate concentrations in the supernatant and cell lysate were upgraded in MLE-12 cells following 1-NP cultivation (Fig. 3R, S). However, the content of acetyl-CoA did not change in MLE-12 cells following 1-NP processed (Fig. 3T). In addition, the levels of glycolysis-related genes were detected. Supplemental Fig. 3 showed that hypoxia-inducible factor 1α (HIF-1α), HK2, PFKFB3, LDHA, and LDHB were elevated after treatment with 1-NP. However, PKM2 did not change. Fig. 3U showed the glycolysis flowchart.

3.4. 1-NP exposure evoked histone lactylation but not histone acetylation in pulmonary epithelial cells

The effect of exposure to 1-NP on lactylation in pulmonary epithelial cells was analyzed. As illustrated in Fig. 4A-D, chronic 1-NP exposure increased Pan Kla, H3K14la, and H4K12la expression levels in mouse lungs compared with those in the control group. In addition, chronic 1-NP upregulated Pan Kla and H3K14la expressions in MLE-12 cells (Fig. 4E-H). The time effect of acute 1-NP treatment on lactylation was explored in MLE-12 cells. The results suggested that acute 1-NP upregulated Pan Kla and H3K14la expressions at 12 h, and the levels remained elevated at 24 h. However, acute 1-NP did not affect Pan Kac and H3K14ac levels in MLE-12 cells (Fig. 4I-L; Supplemental Fig. 4A and B). The dosage impact of acute 1-NP on lactylation was subsequently estimated in MLE-12 cells. The data revealed that the higher the dosage of 1-NP was, the greater the Pan Kla and H3K14la levels were. Similarly, there was no influence of 1-NP on Pan Kac or H3K14ac in MLE-12 cells (Fig. 4M-P; Supplemental Fig. 4C and D). Moreover, IF suggested that exposure to 1-NP raised the counts of Pan Kla- and H3k14la-positive cells in lung tissues and MLE-12 cells (Supplemental Fig. 4E–L).

3.5. 1-NP exposure induced cell cycle arrest and cellular senescence through histone lactylation in pulmonary epithelial cells

Lactate production is determined mainly by LDH (Fig. 5A). Therefore, the effect of *LDHA* knockdown on lactate production was explored

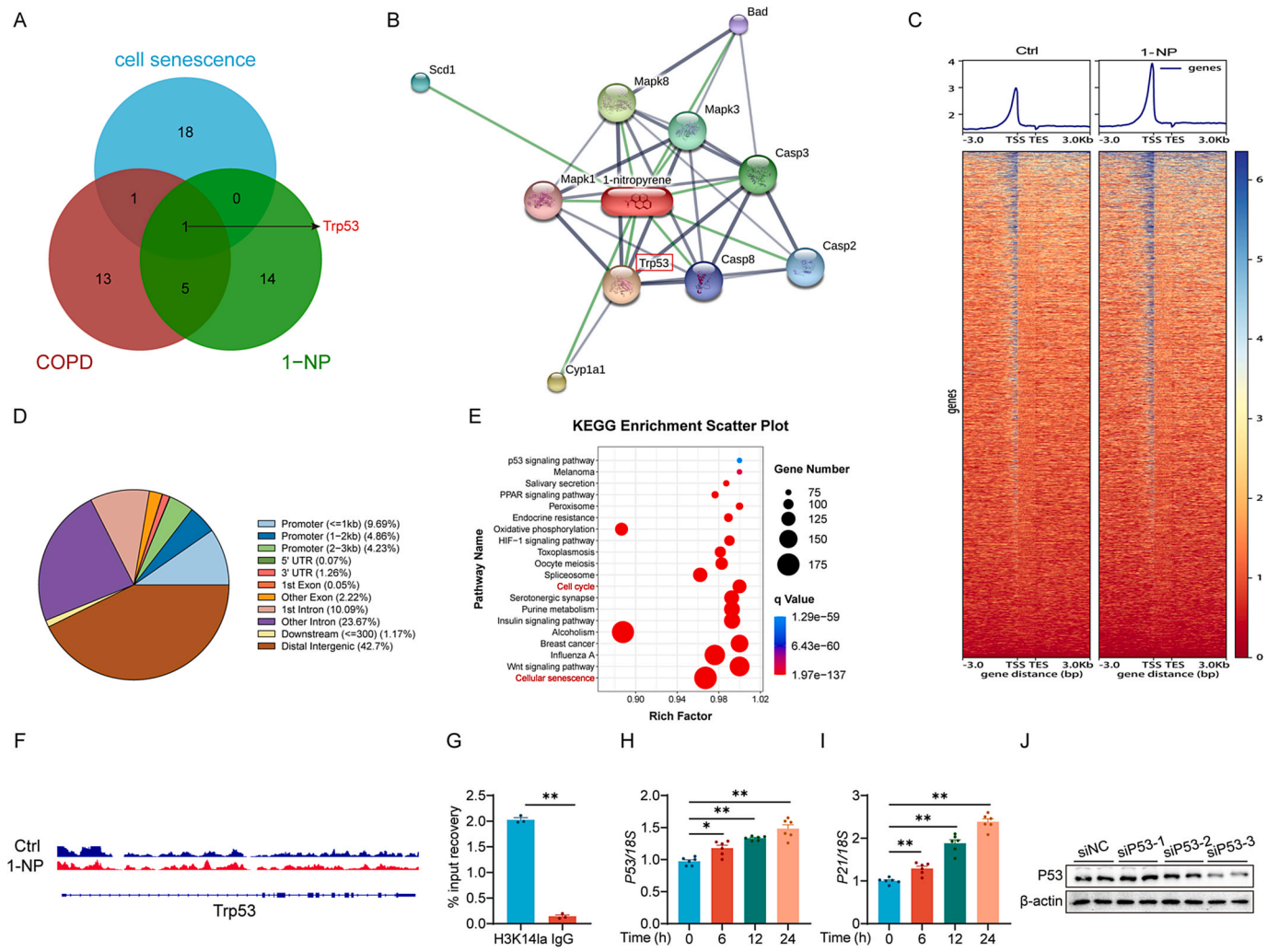

Fig. 6. Histone lactylation activated *p53* transcription in pulmonary epithelial cells. (A) 1-NP-affected genes, COPD-related genes, and senescence-associated genes were analyzed via a Venn diagram. (B) The proteins affected by 1-NP exposure were predicted. (C) The heatmap revealed the binding density of H3K14la, among which existed distinct binding peaks of H3K14la in the 1-NP group and the control group, sorted by signal intensity. (D) A pie chart showed the genomic distribution of H3K14la peaks in the 1-NP group. (E) The bubble plot revealed the KEGG analysis of the increased binding peak of H3K14la in the 1-NP group. (F) IGV tracked for Trp53-enriched in the genomic positions. (G) ChIP-qPCR was used to analyze the binding efficiency of H3K14la to the *p53* promoter region. (H, I) The levels of mRNAs associated with cell cycle arrest were detected via RT-qPCR. (H) *P53*. (*I*) P21. (J-N) The impact of *p53* knockdown on 1-NP-evoked cell cycle arrest was evaluated in MLE-12 cells. (J, K) The effect of *p53* siRNA on p53 protein expression was assessed. (L, M) P21 protein expression was determined by western blotting and quantified. (N) *P21* mRNA expression was evaluated by RT-qPCR. (O, P) The effect of *p53* siRNA on 1-NP-induced cell cycle arrest was explored. (O) Cell cycle distribution was determined by flow cytometry. (P) Cell cycles distribution was analyzed. (Q-R) The effect of *p53* knockdown on 1-NP-triggered premature senescence was estimated in MLE-12 cells. (Q) Senescent cells were detected via SA-β-gal staining. Original magnifications: 100 × and 400 × . (R) The number of SA-β-gal-positive cells was calculated. (S-W) The mRNA levels of SASP components were measured via RT-qPCR. (S) *Il-1β*. (T) *Il-6*. (U) *Tnf-α*. (V) *Mmp-2*. (W) *Cxcl-9*. All the data were expressed as the means ± S.E.M. (N=6). $^{*}P < 0.05$, $^{**}P < 0.01$.

in MLE-12 cells. As shown in Fig. 5B and 5C, *LDHA* siRNA transfection obviously decreased LDHA protein expression in MLE-12 cells, and the most efficacious sequences were siLDHA-2 and siLDHA-3. Pretreatment with siLDHA dramatically mitigated 1-NP-provoked lactate production in MLE-12 cells and supernatants (Fig. 5D, E). Additionally, the 1-NP-induced increase in overall lactylation and H3K14la levels were attenuated by siLDHA transfection, whereas total acetylation and H3K14ac levels were not affected (Fig. 5F-H). IF also confirmed that siLDHA transfection repressed 1-NP-mediated increase in H3K14la-positive cells (Fig. 5I, J). The impacts of siLDHA transfection on cell cycle arrest and senescence caused by 1-NP were subsequently assessed in MLE-12 cells. As shown in Fig. 5K and 5L, LDHA knockdown downregulated 1-NP-induced increase in SA-β-gal-positive cells. Moreover, siLDHA transfection obviously restored 1-NP-provoked upregulation of p21 and p53 expressions, and the decrease in Lamin B1 expression (Fig. 5M-P). Similarly, 1-NP-induced increase in p53 and p21 mRNA levels was inhibited by siLDHA transfection (Fig. 5Q, R). In addition, siLDHA transfection obviously abolished 1-NP-evoked p53 nuclear translocation in MLE-12 cells (Fig. 5S, T). In addition, flow cytometry revealed that 1-NP-induced cell cycle arrest in the S and G2/M phases was inhibited by siLDHA transfection (Fig. 5U, V). Moreover, 1-NP-induced SASP upregulation was obviously mitigated in the 1-NP + siLDHA group (Fig. 5W).

3.6. 1-NP exposure increased p53 transcription through histone H3 lysine 14 lactylation

It is well-known that histone modifications can influence the transcriptional activity and promote the expression of target genes. In order to investigate the plausible mechanism of H3K14la-mediated cell senescence, the top 20 genes related to cellular senescence from the

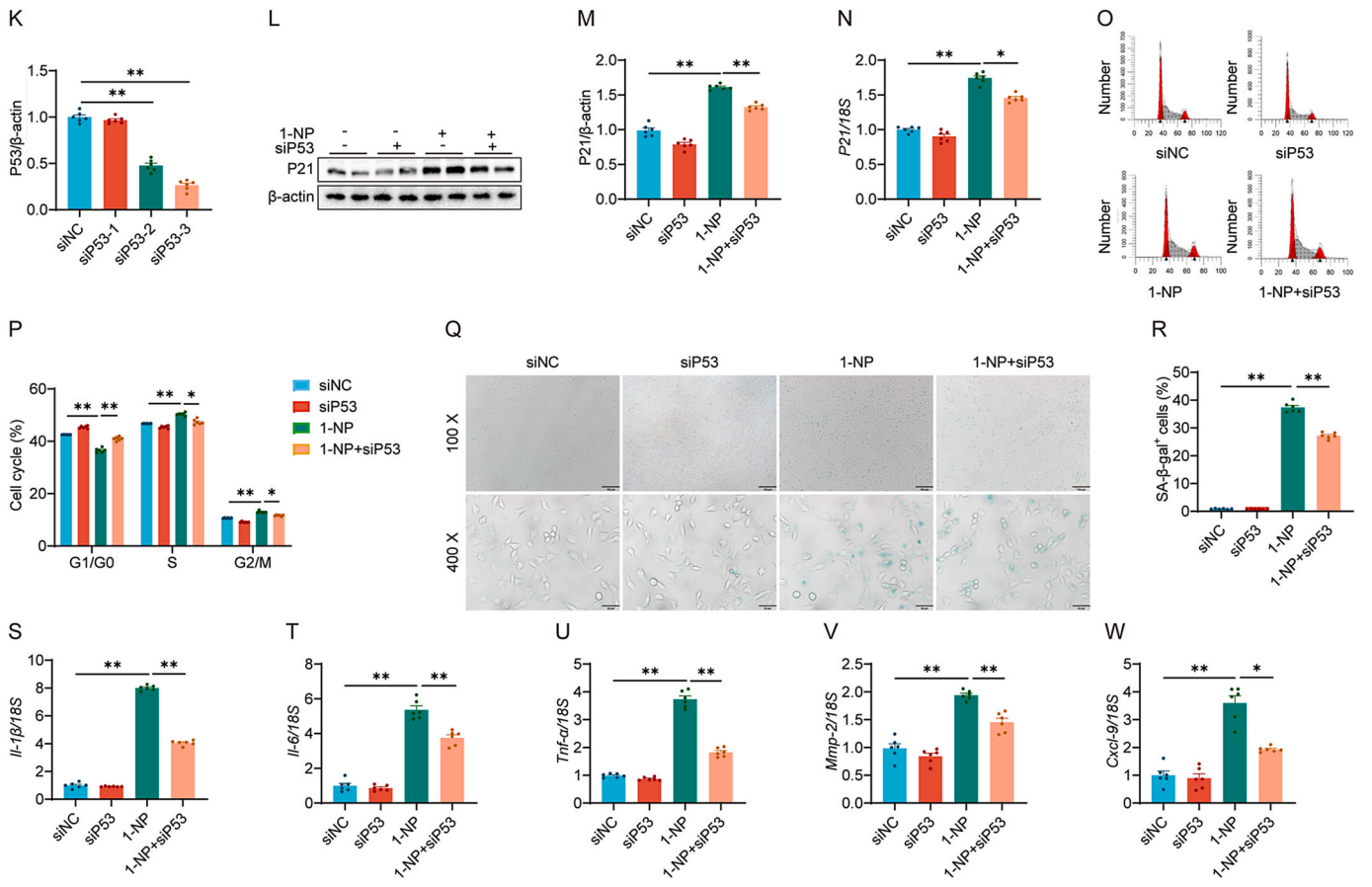

Fig. 6. (*continued*).

GeneCards database (http://www.genecards.org/) and the top 20 genes of the interacting with 1-NP-affected and COPD-related to genes from the CTD website (http://ctdbase.org/) were analyzed using a Venn diagram. As illustrated in Fig. 6A, there was merely one mutually intersected gene, namely Trp53. Moreover, the Stitch website (http://stitch.embl.de/) predicted that 1-NP exposure may affect the expressions of potential proteins, and p53 was also a target protein (Fig. 6B). Then, CUT&Tag assay was conducted. The results showed that 1-NP-induced significant aggregation of H3K14la peaks (Fig. 6C), among which 11,166 (21.75 %) H3K14la binding peaks were located within the promoter region (≤ 3 kb) (Fig. 6D). KEGG analysis revealed that H3K14la-regulated genes were significantly enriched in the signaling pathways of p53, cell cycle, and senescence in the 1-NP-exposed cells (Fig. 6E). Compared to the control group, H3K14la signal was significantly enriched at the *p53* promoter of 1-NP group (Fig. 6F). Meanwhile, ChIP-qPCR further revealed that H3K14la was enriched at the *p53* promoter in pulmonary epithelial cells (Fig. 6G). As presented in Fig. 6H and I, 1-NP increased *p53* and *p21* mRNA levels from 6 h to 24 h in MLE-12 cells. In addition, p53 protein expression was significantly reduced after transfection with p53 siRNA (Fig. 6J, K). As expected, pretreatment with p53 siRNA obviously attenuated 1-NP-induced increases in p21 protein and mRNA expressions (Fig. 6L-N). In addition, flow cytometry suggested that p53 siRNA alleviated 1-NP-induced cell cycle arrest (Fig. 6O, P) and cellular senescence (Fig. 6Q, R). Moreover, p53 knockdown inhibited the secretion of 1-NP-induced SASP proteins, including *Il-1β*, *Il-6*, *Tnf-α*, *Mmp-2*, and *Cxcl-9* (Fig. 6S-W). In addition, the expressions of p53 with H3K14la were evaluated and confirmed in COPD patients and age- and sex- matched control volunteers via a case-control study. The results indicated that the expressions of p53 and H3K14la were obviously elevated in lung tissues of COPD patients compared with control subjects (Supplemental Fig. 5A and B). Not only that, Pearson Correlative analysis found the significant and positive correlation between p53 and H3K14la in COPD patients (R=0.671; *P*=0.020) (Supplemental Fig. 5C). Further analysis revealed that the expressions of p53 and H3K14la were higher in COPD patients with smoke compared with nonsmoker (Supplemental Fig. 5D).

3.7. *Pharmacological inhibition of lactate production mitigated 1-NP-induced cell cycle arrest and senescence in mouse lungs*

The impact of lactate production repression on 1-NP-induced histone lactylation was assessed in mouse lungs. The results revealed that OXA pretreatment alleviated chronic 1-NP-evoked lactate production in serum and lung tissues (Fig. 7A, B). Moreover, pretreatment with OXA attenuated chronic 1-NP-induced upregulation of Pan Kla and H3K14la in mouse lungs (Fig. 7C-F). In addition, pretreatment with OXA repressed 1-NP-induced increase in H3K14la-positive cells in mouse lungs (Fig. 7G, H). The influences of lactate production inhibition on 1-NP-induced cell cycle arrest and senescence were subsequently evaluated in mouse lungs. The results indicated that chronic 1-NP-mediated increase in SA-β-gal-positive cells was inhibited in mouse lungs by OXA pretreatment (Fig. 7I, K). Additionally, chronic 1-NP-induced increases in p53-positive nuclei were mitigated in 1-NP + OXA mice (Fig. 7J, L). Encouragingly, chronic 1-NP-mediated upregulation of p53 and p21, as well as downregulation of Lamin B1, were restored by OXA pretreatment in mouse lungs (Fig. 7M-P). Similarly, pretreatment with OXA alleviated chronic 1-NP-induced increase in *p53* and *p21* mRNA levels (Fig. 7Q, R) and the number of p21-positive cells (Fig. 7S, T) in mouse lungs. Finally, the effect of lactate production inhibition on chronic 1-NP-induced increase in the SASP was estimated in mouse lungs. As shown in Fig. 7U, OXA pretreatment markedly repressed the SASP upregulation induced by 1-NP.

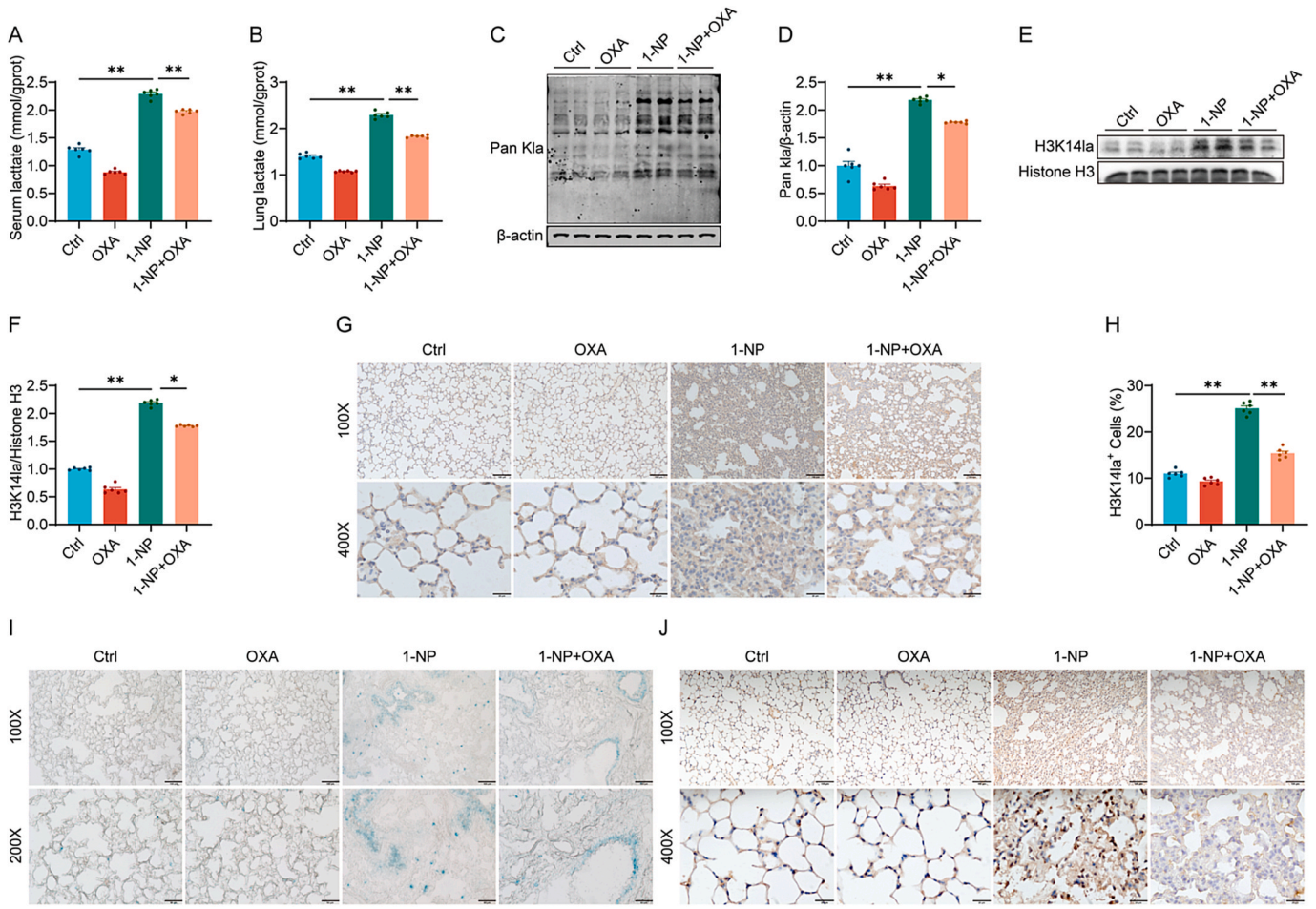

Fig. 7. OXA supplementation alleviated 1-NP-triggered cell cycle arrest and cellular senescence in mouse lungs. (A-H) The effect of OXA supplementation on 1-NP-mediated histone lactylation was analyzed in mice. In the OXA and 1-NP + OXA groups, the mice were pretreated with OXA (100 mg/kg) through intraperitoneal injection. In the 1-NP and 1-NP + OXA groups, the mice were exposed to 1-NP aerosol (200 mg/L, 4 h/day, once every 2 days). Four months after 1-NP exposure, all the mice were harvested, and histone lactylation was measured in the lungs. (A) Serum lactate level was measured. (B) Pulmonary lactate level was quantified. (C, D) Pan Kla protein expression was detected via western blotting and quantified. (E, F) H3K14la protein expression was detected via western blotting and quantified. (G, H) The number of H3K14la-positive nuclei was assessed via IHC and analyzed. Original magnification: 100 × and 400 × . (I-S) The influences of OXA supplementation on 1-NP-induced cell cycle arrest and premature senescence were explored in mouse lungs. (I, K) Senescent cells were evaluated by SA-β-gal staining and the number of SA-β-gal-positive cells was calculated. Original magnifications: 100 × and 400 × . (J, L) The number of p53-positive nuclei was measured via IHC and calculated. Original magnification: 100 × and 400 × . (M) The protein expression of cell cycle markers was assessed by western blotting. (N-P) Quantitative analysis was performed. (N) Lamin B1. (O) P53. (P) P21. (Q, R) The mRNA levels of cell cycle markers were detected via RT-qPCR. (Q) *P53*. (R) *P21*. (S, T) The number of p21-positive cells was detected via IF and calculated. Original magnification: 630 × . (U) The mRNA levels of SASP factors were detected by RT-qPCR. All the data were expressed as the means ± S.E.M. (N=6). $^{*}P < 0.05$, $^{**}P < 0.01$.

3.8. Pharmacological inhibition of lactate production alleviated the 1-NP-induced COPD-like phenotype in mice

The effect of OXA on the 1-NP-induced COPD-like phenotype was analyzed in mice. As shown in Fig. 8A-C, although OXA pretreatment had no effect on the chronic 1-NP-induced decrease in body weight, chronic 1-NP-mediated increase in lung weight and lung coefficient were obviously attenuated by OXA pretreatment. Furthermore, supplementation with OXA relieved chronic 1-NP-evoked COPD-like alveolar structural damage and airway obstruction (Fig. 8D, E). In addition, OXA supplementation obviously decreased airway wall area, the mean linear intercept, airway wall thickness, inflammatory cell infiltration and pathological scores increment in mouse lungs (Fig. 8F-J). Finally, the effect of OXA supplementation on the decrease in pulmonary function induced by chronic 1-NP was analyzed. As expected, the decreases in FVC, FEV1, FEV1/FVC%, and PEF induced by chronic 1-NP were all alleviated in 1-NP + OXA mice (Fig. 8K-N).

4. Discussion

The present investigation explored the impact of chronic 1-NP exposure on COPD in mice and on the senescence in pulmonary epithelial cells. The significantly innovative findings were as follows: (1) 1-NP exposure induced a COPD-like phenotype in mice; (2) 1-NP exposure increased p53 transcription, promoted cell cycle arrest, and induced premature senescence in mouse lungs and pulmonary epithelial cells; (3) 1-NP exposure promoted glycolysis and lactate production in pulmonary epithelial cells; (4) 1-NP exposure triggered histone lactylation in pulmonary epithelial cells; (5) 1-NP exposure upregulated *p53* transcription through H3K14la; and (6) Pharmacological inhibition of lactate production attenuated 1-NP-mediated cell cycle arrest and premature senescence in pulmonary epithelial cells, as well as the COPD-like phenotype in mice.

Cellular senescence is characterized by cell cycle arrest, altered cell morphology, telomere shortening, increased SASP, etc. [24,44]. Several studies have demonstrated that cellular senescence is involved in COPD

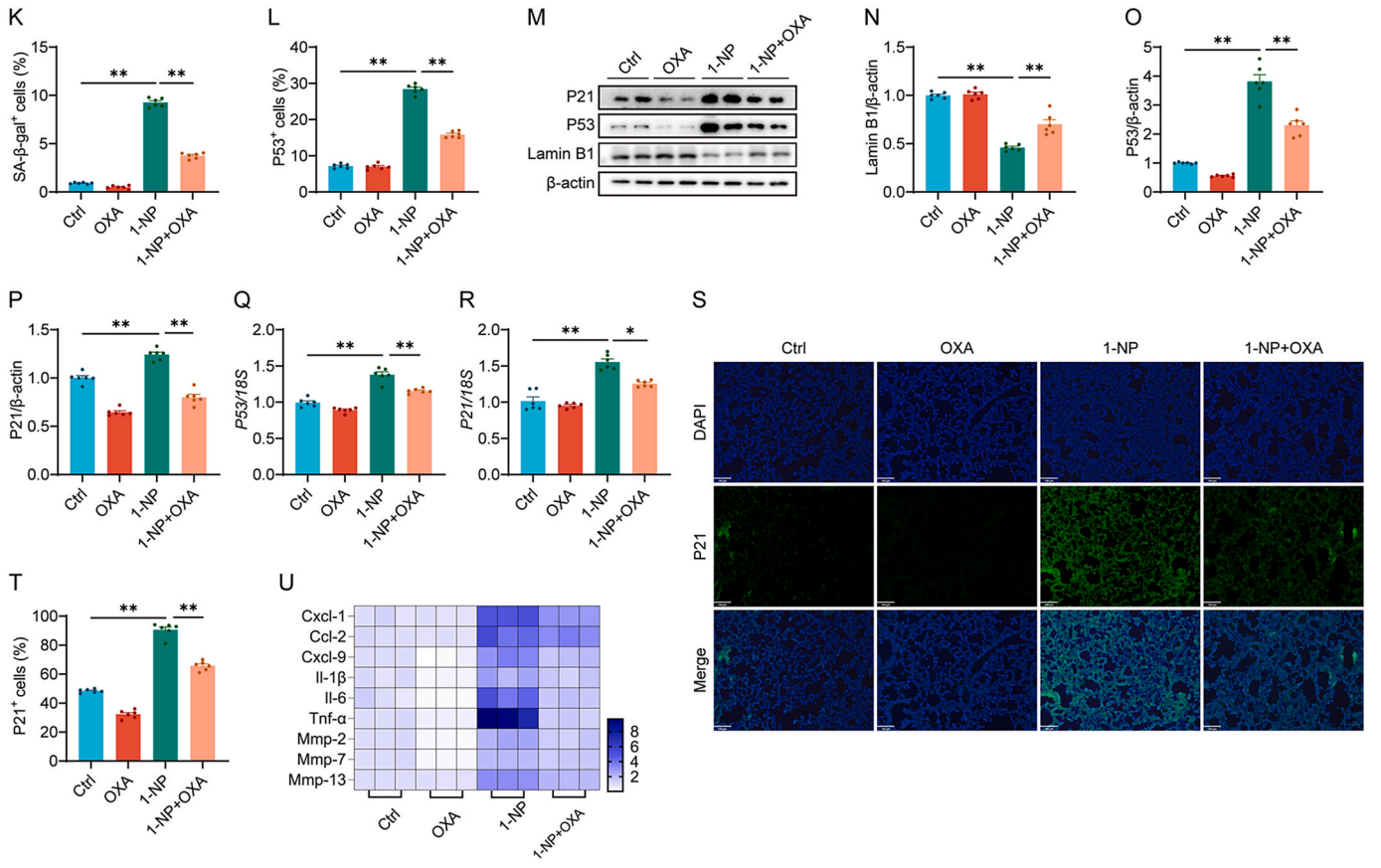

Fig. 7. (*continued*).

progression [29,45]. In previous research from our laboratory, 1-NP provokes telomere damage and cellular senescence in the progression of pulmonary fibrosis [30]. Therefore, we hypothesized that chronic 1-NP exposure may cause COPD through premature senescence in pulmonary epithelial cells. Our animal experiments revealed that chronic 1-NP exposure resulted in alveolar structural damage, increased inflammation, decreased pulmonary function, and a COPD-like phenotype in mice. In addition, in vivo and in vitro experiments revealed that 1-NP exposure induced cell cycle arrest and premature senescence in mouse lungs and MLE-12 cells. Therefore, these outcomes suggest that chronic 1-NP exposure triggers COPD through initiating cell cycle arrest and premature senescence in pulmonary epithelial cells.

P53 is recognized as a powerful transcription factor that plays an important role in tumor suppression and cellular response to stress [44,46]. Recent studies have shown that p53 is involved in deciding the cellular fate and impacting the cell cycle. The activation of p53 can transcriptionally upregulate p21, inhibit many cell cycle genes, and ultimately induce cell cycle arrest [47,48]. Moreover, p53 nuclear translocation promotes *p21* transcription and cellular senescence [49]. Not only that, p53 posttranslational modification also exerts significate roles on regulating p53 activation and cellular senescence in different cell types. UFMylation, a recently found ubiquitin-like modification, stabilizes p53 via repressing p53 ubiquitination degradation and then facilities *p21* transcription in human renal epithelial cells [50]. Moreover, p53 acetylation upregulates p21 expression and incurs cell cycle arrest in human diploid fibroblast line [51]. A recent study found that p53 SUMOylation provokes p53 phosphorylation, and upregulates the transcriptional activity of p53 and excites senescence in neurons [52]. Therefore, these results all hinted that p53 activation is implicated in the process of cellular senescence. In the present study, we found that 1-NP exposure increased p53 mRNA and protein expressions, activated the p53/p21 signaling axis and downregulated the expressions of cell cycle-related genes in mouse lungs and MLE-12 cells. Additional, p53 knockdown obviously relieved 1-NP-mediated cell cycle arrest and senescence in MLE-12 cells. Hence, p53 activation-mediated cell cycle arrest is involved in pulmonary epithelial cell senescence during 1-NP-induced COPD. However, the mechanism by which 1-NP activates the p53 transcription factor in pulmonary epithelial cells is unknown.

Recent research revealed that histone lactylation, as a new epigenetic modification, regulates gene transcription and cellular senescence [33,34]. Therefore, the impact of histone lactylation on cellular senescence was explored in pulmonary epithelial cells. The results revealed that the lactate levels were significantly increased in the mouse lungs and MLE-12 cells after 1-NP. Gene knockdown and pharmacological inhibition of lactate production all alleviated histone lactylation, p53 activation, cell cycle arrest, and premature senescence in mouse lungs and MLE-12 cells. Moreover, CUT&Tag and ChIP-qPCR experiments confirmed that H3K14la was enriched at the *p53* promoter and directly regulated *p53* transcription in MLE-12 cells. Increased pyruvate can be converted to acetyl-CoA and lactyl-CoA [53,54]. Elevated acetyl-col levels induce histone acetylation and regulate gene transcription [55,56]. Therefore, the effect of histone acetylation on *p53* upregulation needs to be eliminated. According to our findings, 1-NP exposure in MLE-12 cells only raised lactate levels, not acetyl-CoA. In addition, acute 1-NP did not evoke H3K14ac in mouse lungs and MLE-12 cells. These findings demonstrate that exposure to 1-NP induces cell cycle arrest and premature senescence through H3K14la, which positively regulates *p53* transcription in pulmonary epithelial cells. It was reported that H4K12la upregulates the transcription of SASP genes and drives smooth muscle cell senescence [34]. In addition, H4K12la activates NF-κB signaling via enhancing binding to the promoters of NF-κB p65 and p50, and then incurs cellular senescence [57]. These results hinted that there are other proteins lactylation which drive cellular senescence. Therefore, the roles of the more proteins lactylation on 1-NP-induced senescence will be

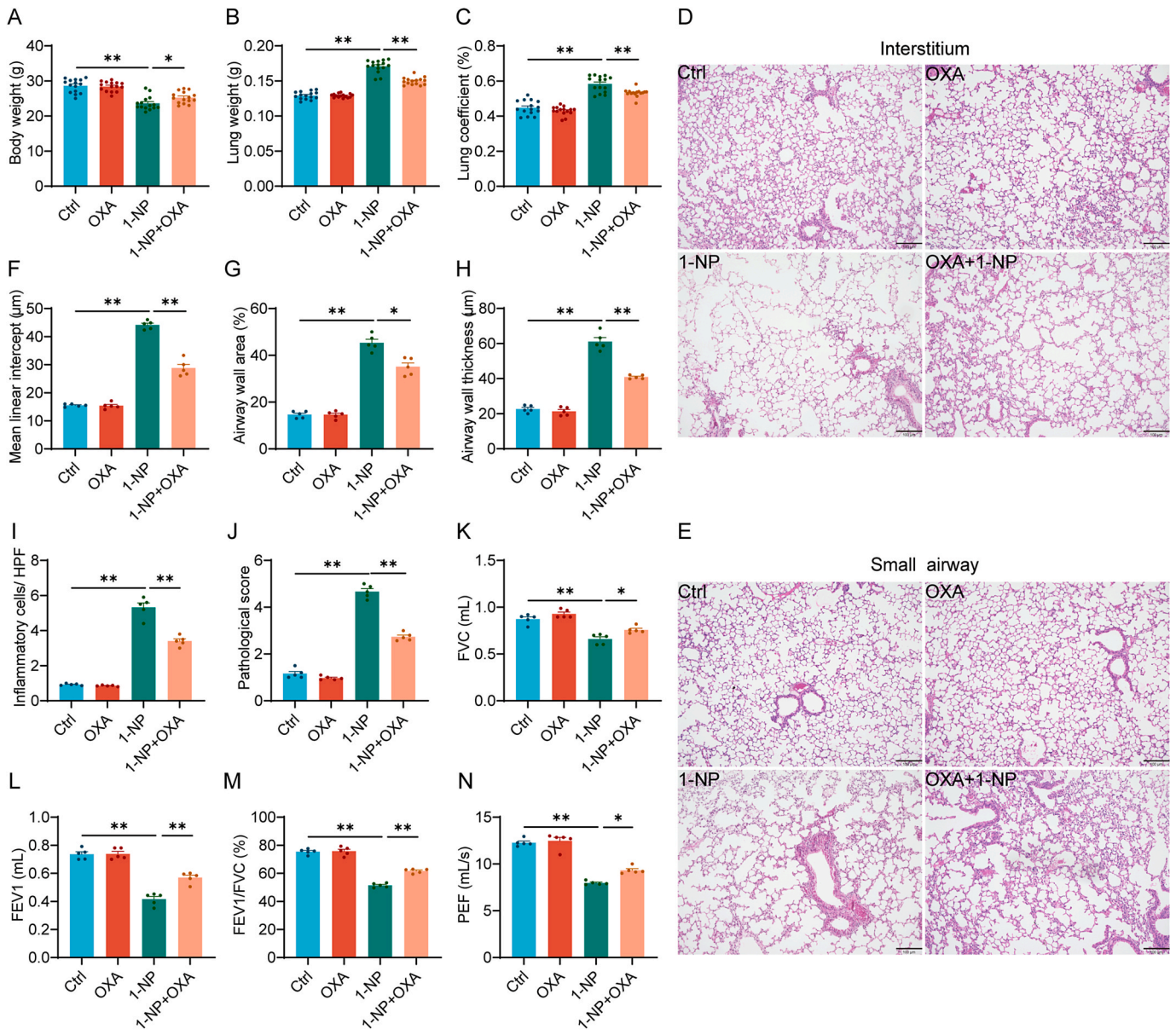

Fig. 8. OXA supplementation attenuated 1-NP-evoked a COPD-like phenotype in mice. (A-N) The effect of OXA supplementation on 1-NP-induced COPD was analyzed in mice. In the OXA and 1-NP + OXA groups, the mice were supplemented with OXA (100 mg/kg) through intraperitoneal injection. In the 1-NP and 1-NP + OXA groups, the mice were exposed to 1-NP aerosol (200 mg/L, 4 h/day, once every 2 days). Four months after 1-NP exposure, all the mice were harvested, pulmonary function was tested and lung tissues were collected. (A) Body weight. (B) Lung weight. (C) Lung coefficient. (D-E) The lung interstitium and small airways were stained with hematoxylin and eosin. Original magnification: 400 × . (F) Mean linear intercept. (G) Airway wall area. (H) Airway wall thickness. (I) Inflammatory cells. (J) Pathological scores. (K-N) Pulmonary function was measured. (K) FVC. (L) FEV1. (M) FEV1/FVC. (N) PEF. All the data were expressed as the means ± S.E.M. (N=6). $^{*}P < 0.05$, $^{**}P < 0.01$.

explored in pulmonary epithelial cells in the next investigation.

Lactate, an end product of glycolysis, was initially thought to be a metabolic waste product. However, increasing evidence has suggested that lactate can be used as a metabolic fuel for normal tissues and to determine cell fate [58,59]. Additionally, several studies have suggested that lactate acts as a signaling molecule with different regulatory functions, including cellular homoeostasis modulation and lipolysis [60,61]. In the process of glycolysis, under both anaerobic and aerobic conditions, pyruvate is converted to lactate by LDH [62]. Elevated levels of lactate bind to the lysine of histones and evoke histone lactylation, which regulates gene transcription [33]. In this study, three key glycolytic enzymes, HK2, PFKFB3, and PKM2, were upregulated in 1-NP-exposed mouse lungs and MLE-12 cells. In addition, 1-NP exposure significantly elevated LDHA and lactate levels in pulmonary epithelial cells. As predicted, LDHA siRNA and oxamate, which are inhibitors of LDHA, attenuated lactate production and histone lactylation in pulmonary epithelial cells. Further investigations revealed that LDHA knockdown and pharmacological inhibition relieved 1-NP-mediated cell cycle arrest and premature senescence in pulmonary epithelial cells. In addition, supplementation with oxamate effectively repressed 1-NP-induced COPD in mice. Collectively, these findings demonstrated that exposure to 1-NP exacerbates lactate production through upregulating glycolysis and LDHA expression in pulmonary epithelial cells.

The two important clinical phenotypes of COPD are emphysema and bronchiolitis [63]. The previous studies have revealed that airway inflammation and remodeling exert important roles in the occurrence and development of COPD [64,65]. Additionally, cellular senescence in pulmonary epithelial cells and fibroblasts are observed in CS-induced

the progression of emphysema [66], hinting these phenotypes have different mechanisms in COPD. However, due to the limitation of actual situation and experimental funding, only the effects of 1-NP exposure on senescence and histone lactylation were evaluated in pulmonary epithelial cells in our research. The knowledge of 1-NP exposure on other types of cells were obscure. These mechanisms were not confirmed in other cell models. This was a research flaw. The current results may restrict the promotion of the findings. So, the influences of 1-NP exposure will be further explored in other types of cells next.

5. Conclusion

In conclusion, this study revealed that chronic exposure to 1-NP, a prevalent environmental pollutant, results in the initiation of COPD through evoking cell cycle arrest and premature senescence in pulmonary epithelial cells. Additionally, 1-NP exposure promotes lactate production and histone lactylation via upregulating glycolysis and LDHA expression in pulmonary epithelial cells. Mechanistically, elevated lactate positively regulates *p53* transcription through H3K14la and promotes to cell cycle arrest and then premature senescence in pulmonary epithelial cells. Conversely, the inhibition of lactate production attenuates 1-NP-mediated H3K14la, cell cycle arrest, premature senescence, and COPD. These results indicate that glycolysis-derived lactate and H3K14la may be the potential therapeutic targets for COPD progression via repressing cell cycle arrest and premature senescence in pulmonary epithelial cells. Our data provide a novel approach for inhibiting environmental pollutant-mediated COPD in the future.

CRediT authorship contribution statement

Rong-Rong Wang: Project administration, Methodology. **Dan-Lei Chen:** Writing – review & editing, Project administration. **Meng Wei:** Supervision. **Se-Ruo Li:** Project administration, Methodology. **Peng Zhou:** Supervision. **Jing Sun:** Methodology. **Qi-Yuan He:** Methodology. **Jin Yang:** Supervision, Conceptualization. **Hui Zhao:** Writing – review & editing, Conceptualization. **Lin Fu:** Writing – original draft, Supervision, Conceptualization.

Declaration on research ethics

This study was approved by the Association of Laboratory Animal Sciences at Anhui Medical University (LLSC20220026), and verification of approval is available upon request.

Declaration of competing interest

The authors declare that they have no known competing financial interests or personal relationships that could have appeared to influence the work reported in this paper.

Acknowledgements

This study was supported by the National Natural Science Foundation of China (82270071, 82100078), Anhui Provincial Clinical Research Transformation Project (202204295107020014, 202204295107020056), Research Funds of Center for Big Data and Population Health of IHM (JKS2022007, JKS2023010), University Natural Science Research Project of Anhui Province (2023AH030117).

Appendix A. Supplementary data

Supplementary data to this article can be found online at https://doi.org/10.1016/j.redox.2025.103703.

Data availability

Data will be made available on request.

References

[1] B. Bandowe, H. Meusel, Nitrated polycyclic aromatic hydrocarbons (nitro-PAHs) in the environment - a review, Sci. Total Environ. 581–582 (2017) 237–257.
[2] Y. Gao, L. Yang, J. Chen, Y. Li, P. Jiang, J. Zhang, et al., Nitro and oxy-PAHs bounded in $PM_{2.5}$ and $PM_{1.0}$ under different weather conditions at Mount Tai in Eastern China: sources, long-distance transport, and cancer risk assessment, Sci. Total Environ. 622–623 (2018) 1400–1407.
[3] K. Deng, W. Chan, Development of a QuEChERS-based method for determination of carcinogenic 2-nitrofluorene and 1-nitropyrene in rice grains and vegetables: a comparative study with benzo[a]pyrene, J. Agric. Food Chem. 65 (9) (2017) 1992–1999.
[4] S.J. Feng, X.B. Shen, X.W. Hao, X.Y. Cao, X. Li, X.L. Yao, et al., Polycyclic and nitro-polycyclic aromatic hydrocarbon pollution characteristics and carcinogenic risk assessment of indoor kitchen air during cooking periods in rural households in North China, Environ. Sci. Pollut. Res. Int. 28 (9) (2021) 11498–11508.
[5] Y. Wang, M. Adgent, P.H. Su, H.Y. Chen, P.C. Chen, C.A. Hsiung, et al., Prenatal exposure to perfluorocarboxylic acids (PFCAs) and fetal and postnatal growth in the taiwan maternal and infant cohort study, Environ. Health Perspect. 124 (11) (2016) 1794–1800.
[6] D. Yaffe, Y. Cohen, J. Arey, A.J. Grosovsky, Multimedia analysis of PAHs and nitro-PAH daughter products in the Los Angeles Basin, Risk, Anal. 21 (2) (2001) 275–294.
[7] I.C. Yadav, N.L. Devi, V.K. Singh, J. Li, G.Z. hang, Concentrations, sources and health risk of nitrated- and oxygenated-polycyclic aromatic hydrocarbon in urban indoor air and dust from four cities of Nepal, Sci. Total Environ. 643 (2018) 1013–1023.
[8] K.K. Stenerson, O. Shimelis, M.R. Halpenny, K. Espenschied, M.M. Ye, Analysis of polynuclear aromatic hydrocarbons in olive oil after solid-phase extraction using a dual-layer sorbent cartridge followed by high-performance liquid chromatography with fluorescence detection, J. Agric. Food Chem. 63 (20) (2015) 4933–4939.
[9] L. Benbrahim-Tallaa, R. Abaan, Y. Grosse, B. Lauby-Secretan, F. El Ghissassi, V. Bouvard, et al., Carcinogenicity of diesel-engine and gasoline-engine exhausts and some nitroarenes, Lancet Oncol. 13 (7) (2012) 663–664.
[10] M.J. Edwards, S. Batmanghelich, S. Edwards, J.M. Parry, K. Smith, The induction of DNA adducts in mammalian cells exposed to 1-nitropyrene and its nitro-reduced derivatives, Mutagenesis 1 (5) (1986) 347–352.
[11] Y.X. Liang, Q.Z. Shuai, Y. Wang, S.S. Jin, Z.H. Feng, B.H. Chen, et al., 1-Nitropyrene exposure impairs embryo implantation through disrupting endometrial receptivity genes expression and producing excessive ROS, Ecotoxicol. Environ. Saf. 227 (2021) 112939.
[12] X.L. Li, Y.L. Liu, J.Y. Liu, Y.Y. Zhu, X.X. Zhu, W.W. Zhang, et al., 1-Nitropyrene disrupts testicular steroidogenesis via oxidative stress-evoked PERK-eIF2α pathway, Ecotoxicol. Environ. Saf. 259 (2023) 115027.
[13] R. Li, X.L. Wang, B. Wang, J. Li, Y.P. Song, B. Luo, et al., Gestational 1-nitropyrene exposure causes fetal growth restriction through disturbing placental vascularity and proliferation, Chemosphere 213 (2018) 252–258.
[14] X. Lu, Z.X. Tan, B. Wang, J. Li, B. Hu, L. Gao, et al., Maternal 1-nitropyrene exposure during pregnancy increases susceptibility of allergic asthma in adolescent offspring, Chemosphere 243 (2020) 125356.
[15] L. Fu, H. Zhao, Y. Xiang, H.X. Xiang, B. Hu, Z.X. Tan, et al., Reactive oxygen species-evoked endoplasmic reticulum stress mediates 1-nitropyrene-induced epithelial-mesenchymal transition and pulmonary fibrosis, Environ. Pollut. 283 (2021) 117134.
[16] B. Hu, B. Tong, Y. Xiang, S.R. Li, Z.X. Tan, H.X. Xiang, et al., Acute 1-NP exposure induces inflammatory responses through activating various inflammatory signaling pathways in mouse lungs and human A549 cells, Ecotoxicol. Environ. Saf. 189 (2020) 109977.
[17] S.A. Christenson, B.M. Smith, M. Bafadhel, N. Putcha, Chronic obstructive pulmonary disease, Lancet 399 (10342) (2022) 2227–2242.
[18] GBD Chronic Respiratory Disease Collaborators, Prevalence and attributable health burden of chronic respiratory diseases, 1990-2017: a systematic analysis for the Global Burden of Disease Study 2017, Lancet Respir. Med. 8 (6) (2020) 585–596.
[19] C. Wang, J. Xu, L. Yang, Y. Xu, X. Zhang, C. Bai, et al., China Pulmonary Health Study Group. Prevalence and risk factors of chronic obstructive pulmonary disease in China (the China Pulmonary Health [CPH] study): a national cross-sectional study, Lancet 391 (10131) (2018) 1706–1717.
[20] J. Xu, Z.L. Ji, P. Zhang, T. Chen, Y. Xie, J. Li, Disease burden of COPD in the Chinese population: a systematic review, Ther. Adv. Respir. Dis. 17 (2023) 17534666231218899.
[21] N. Zhong, C. Wang, W. Yao, P. Chen, J. Kang, S. Huang, et al., Prevalence of chronic obstructive pulmonary disease in China: a large, population-based survey, Am. J. Respir. Crit. Care Med. 176 (8) (2007) 753–760.
[22] D.D. Sin, D. Doiron, A. Agusti, A. Anzueto, P.J. Barnes, B.R. Celli, et al., GOLD Scientific Committee. Air pollution and COPD: GOLD 2023 committee report, Eur. Respir. J. 61 (5) (2023) 2202469.
[23] M. Ogrodnik, Cellular aging beyond cellular senescence: markers of senescence prior to cell cycle arrest in vitro and in vivo, Aging Cell 20 (4) (2021) e13338.
[24] J.P. de Magalhães, Cellular senescence in normal physiology, Science 384 (6702) (2024) 1300–1301.

[25] S. Da Silva-Álvarez, P. Picallos-Rabina, L. Antelo-Iglesias, F. Triana-Martínez, A. Barreiro-Iglesias, L. Sánchez, et al., The development of cell senescence, Exp. Gerontol. 128 (2019) 110742.
[26] V. Lucas, C. Cavadas, C.A. Aveleira, Cellular senescence: from mechanisms to current biomarkers and senotherapies, Pharmacol. Rev. 75 (4) (2023) 675–713.
[27] P.L. de Keizer, The fountain of youth by targeting senescent cells? Trends, Mol. Med. 23 (1) (2017) 6–17.
[28] A. Kowald, J.F. Passos, T.B.L. Kirkwood, On the evolution of cellular senescence, Aging Cell 19 (12) (2020) e13270.
[29] J. Araya, K. Tsubouchi, N. Sato, S. Ito, S. Minagawa, H. Hara, et al., PRKN-regulated mitophagy and cellular senescence during COPD pathogenesis, Autophagy 15 (3) (2019) 510–526.
[30] S.R. Li, N.N. Kang, R.R. Wang, M.D. Li, L.H. Chen, P. Zhou, et al., ALKBH5 SUMOylation-mediated FBXW7 m6A modification regulates alveolar cells senescence during 1-nitropyrene-induced pulmonary fibrosis, J. Hazard. Mater. 468 (2024) 133704.
[31] S.W. Wu, C.H. Su, Y.C. Ho, R. Huang-Liu, C.C. Tseng, Y.W. Chiang, et al., Genotoxic effects of 1-nitropyrene in macrophages are mediated through a p53-dependent pathway involving cytochrome c release, caspase activation, and PARP-1 cleavage, Ecotoxicol. Environ. Saf. 213 (2021) 112062.
[32] J. Bleckwedel, F. Mohamed, F. Mozzi, R.R. Raya, Major role of lactate dehydrogenase D-LDH1 for the synthesis of lactic acid in Fructobacillus tropaeoli CRL 2034, Appl. Microbiol. Biotechnol. 104 (17) (2020) 7409–7426.
[33] D. Zhang, Z. Tang, H. Huang, G. Zhou, C. Cui, Y. Weng, et al., Metabolic regulation of gene expression by histone lactylation, Nature 574 (7779) (2019) 575–580.
[34] X. Li, M. Chen, X. Chen, X. He, X. Li, H. Wei, et al., TRAP1 drives smooth muscle cell senescence and promotes atherosclerosis via HDAC3-primed histone H4 lysine 12 lactylation, Eur. Heart J. 45 (39) (2024) 4219–4235.
[35] X. Li, H. Yang, H. Sun, R. Lu, C. Zhang, N. Gao, et al., Taurine ameliorates particulate matter-induced emphysema by switching on mitochondrial NADH dehydrogenase genes, Proc. Natl. Acad. Sci. U. S. A 114 (45) (2017) 9655–9664.
[36] M.D. Li, L.H. Chen, H.X. Xiang, Y.L. Jiang, B.B. Lv, D.X. Xu, et al., Benzo[a]pyrene evokes epithelial-mesenchymal transition and pulmonary fibrosis through AhR-mediated Nrf2-p62 signaling, J. Hazard. Mater. 473 (2024) 134560.
[37] B.Q. Liao, C.B. Liu, S.J. Xie, Y. Liu, Y.B. Deng, S.W. He, et al., Effects of fine particulate matter (PM2.5) on ovarian function and embryo quality in mice, Environ. Int. 135 (2020) 105338.
[38] H. Lin, C. Wang, H. Yu, Y. Liu, L. Tan, S. He, et al., Protective effect of total Saponins from American ginseng against cigarette smoke-induced COPD in mice based on integrated metabolomics and network pharmacology, Biomed. Pharmacother. 149 (2022) 112823.
[39] H. Wu, H. Ma, L. Wang, H. Zhang, L. Lu, T. Xiao, et al., Regulation of lung epithelial cell senescence in smoking-induced COPD/emphysema by microR-125a-5p via Sp1 mediation of SIRT1/HIF-1a, Int. J. Biol. Sci. 18 (2) (2022) 661–674.
[40] G. Matute-Bello, G. Downey, B.B. Moore, S.D. Groshong, M.A. Matthay, A. S. Slutsky, et al., Acute Lung Injury in Animals Study Group. An official American Thoracic Society workshop report: features and measurements of experimental acute lung injury in animals, Am. J. Respir. Cell Mol. Biol. 44 (5) (2011) 725–738.
[41] K.F. Rabe, S. Hurd, A. Anzueto, P.J. Barnes, S.A. Buist, P. Calverley, et al., Global strategy for the diagnosis, management, and prevention of chronic obstructive pulmonary disease: GOLD executive summary, Am. J. Respir. Crit. Care Med. 176 (6) (2007) 532–555.
[42] J. Fei, L. Fu, W. Cao, B. Hu, H. Zhao, J.B. Li, Low vitamin D status is associated with epithelial-mesenchymal transition in patients with chronic obstructive pulmonary disease, J. Immunol. 203 (6) (2019) 1428–1435.
[43] S.X. Ma, G.F. Xie, P. Fang, M.M. Tang, Y.P. Deng, Y.J. Lu, et al., Low 15d-PGJ2 status is associated with oxidative stress in chronic obstructive pulmonary disease patients, Inflamm. Res. 72 (2) (2023) 171–180.
[44] M. Mijit, V. Caracciolo, A. Melillo, F. Amicarelli, A. Giordano, Role of p53 in the regulation of cellular senescence, Biomolecules 10 (3) (2020) 420.
[45] K. Peng, Y.X. Yao, X. Lu, W.J. Wang, Y.H. Zhang, H. Zhao, et al., Mitochondrial dysfunction-associated alveolar epithelial senescence is involved in $CdCl_2$-induced COPD-like lung injury, J. Hazard. Mater. 476 (2024) 135103.
[46] E.R. Kastenhuber, S.W. Lowe, Putting p53 in context, Cell 170 (6) (2017) 1062–1078.
[47] K. Engeland, Cell cycle regulation: p53-p21-RB signaling, Cell Death Differ. 29 (5) (2022) 946–960.
[48] A. Hafner, M.L. Bulyk, A. Jambhekar, G. Lahav, The multiple mechanisms that regulate p53 activity and cell fate, Nat. Rev. Mol. Cell Biol. 20 (4) (2019) 199–210.
[49] J.G. Jackson, V. Pant, Q. Li, L.L. Chang, A. Quintás-Cardama, D. Garza, et al., p53-mediated senescence impairs the apoptotic response to chemotherapy and clinical outcome in breast cancer, Cancer Cell 21 (6) (2012) 793–806.
[50] J. Liu, D. Guan, M. Dong, J. Yang, H. Wei, Q. Liang, et al., UFMylation maintains tumour suppressor p53 stability by antagonizing its ubiquitination, Nat. Cell Biol. 22 (9) (2020) 1056–1063.
[51] P. Yan, Z. Li, J. Xiong, Z. Geng, W. Wei, Y. Zhang, et al., LARP7 ameliorates cellular senescence and aging by allosterically enhancing SIRT1 deacetylase activity, Cell Rep. 37 (8) (2021) 110038.
[52] L. Wan, F. Yang, A. Yin, Y. Luo, Y. Liu, F. Liu, et al., Age-related p53 SUMOylation accelerates senescence and tau pathology in Alzheimer's disease, Cell Death Differ. (2025), https://doi.org/10.1038/s41418-025-01448-0.
[53] J. Qiao, Y. Tan, H. Liu, B. Yang, Q. Zhang, Q. Liu, et al., Histone H3K18 and ezrin lactylation promote renal dysfunction in sepsis-associated acute kidney injury, Adv. Sci. 11 (28) (2024) e2307216.
[54] H. Rho, A.R. Terry, C. Chronis, N. Hay, Hexokinase 2-mediated gene expression via histone lactylation is required for hepatic stellate cell activation and liver fibrosis, Cell Metab. 35 (8) (2023) 1406–1423.
[55] Y. Lin, A. Lin, L. Cai, W. Huang, S. Yan, Y. Wei, et al., ACSS2-dependent histone acetylation improves cognition in mouse model of Alzheimer's disease, Mol. Neurodegener. 18 (1) (2023) 47.
[56] Y. He, S. Wang, S. Liu, D. Qin, Z. Liu, L. Wang, et al., MSL1 promotes liver regeneration by driving phase separation of STAT3 and histone H4 and enhancing their acetylation, Adv. Sci. 10 (23) (2023) e2301094.
[57] L. Wei, X. Yang, J. Wang, Z. Wang, Q. Wang, Y. Ding, et al., H3K18 lactylation of senescent microglia potentiates brain aging and Alzheimer's disease through the NFκB signaling pathway, J. Neuroinflammation 20 (1) (2023) 208.
[58] R. Nikooie, D. Moflehi, S. Zand, Lactate regulates autophagy through ROS-mediated activation of ERK1/2/m-TOR/p-70S6K pathway in skeletal muscle, J. Cell Commun. Signal. 15 (1) (2021) 107–123.
[59] G.A. Dienel, Lactate shuttling and lactate use as fuel after traumatic brain injury: metabolic considerations, J. Cerebr. Blood Flow Metabol. 34 (11) (2014) 1736–1748.
[60] T.Y. Lee, Lactate: a multifunctional signaling molecule, Yeungnam. Univ. J. Med. 38 (3) (2021) 183–193.
[61] K. Ahmed, S. Tunaru, C. Tang, M. Müller, A. Gille, A. Sassmann, et al., An autocrine lactate loop mediates insulin-dependent inhibition of lipolysis through GPR81, Cell Metab. 11 (4) (2010) 311–319.
[62] Y. Xie, H. Hu, M. Liu, T. Zhou, X. Cheng, W. Huang, et al., The role and mechanism of histone lactylation in health and diseases, Front. Genet. 13 (2022) 949252.
[63] H. Liu, H.Y. Tang, J.Y. Xu, Z.G. Pang, Small airway immunoglobulin A profile in emphysema-predominant chronic obstructive pulmonary disease, Chin Med J (Engl). 133 (16) (2020) 1915–1921.
[64] Y. Wang, J. Xu, Y. Meng, I.M. Adcock, X. Yao, Role of inflammatory cells in airway remodeling in COPD, Int. J. Chronic Obstr. Pulm. Dis. 13 (2018) 3341–3348.
[65] C. Brightling, N. Greening, Airway inflammation in COPD: progress to precision medicine, Eur. Respir. J. 54 (2) (2019) 1900651.
[66] R.M. Tuder, J.A. Kern, Y.E. Miller, Senescence in chronic obstructive pulmonary disease, Proc. Am. Thorac. Soc. 9 (2) (2012) 62–63.